

# Realistic Entanglement Swapping and Dense Coding

by

Amjad Hussain



A dissertation submitted to the

Centre for Advanced Mathematics and Physics,  
National University of Sciences and Technology,  
H-12, Islamabad, Pakistan

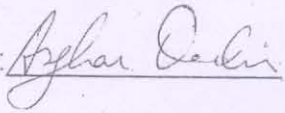

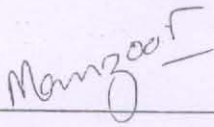
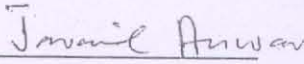
Nov. 2011

**National University of Sciences & Technology****MASTER THESIS WORK**

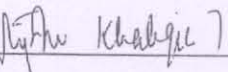
We hereby recommend that the dissertation prepared under our supervision by:

MR. AMJAD HUSSAIN, Regn No. 2009-NUST-MPhil PhD-Phy-01 Titled: Realistic Entanglement Swapping and Quantum Dense Coding be accepted in partial fulfillment of the requirements for the award of **M.Phil** degree.

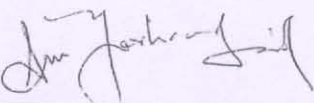
**Examination Committee Members**

- |    |   |   |
|----|---|---|
| 1. | Name: <u>PROF. DR. ASGHAR QADIR</u>     | Signature: <u></u>    |
| 2. | Name: <u>PROF. DR. MUNEER A. RASHID</u> | Signature: <u></u>   |
| 3. | Name: <u>PROF. DR. MANZOOR IKRAM</u>    | Signature: <u></u>  |
| 4. | Name: <u>DR. JAVAID ANWAR</u>           | Signature: <u></u> |

Supervisor's name: DR. AEYSHA KHALIQUE

Signature: 

Date: 30-12-11



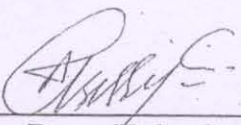
Head of Department

30/12/2011

Date

**COUNTERSIGNED**

Date: 24/01/2012

  
Dean/Principal

# Realistic Entanglement Swapping and Dense Coding

by

Amjad Hussain



A dissertation submitted in the partial fulfillment

for the degree of Master of Philosophy

in

Physics

Supervised by

Dr. Aeysha Khalique

Centre for Advanced Mathematics and Physics,

National University of Sciences and Technology,

H-12, Islamabad, Pakistan

# Abstract

In this dissertation two quantum information processes are studied, entanglement swapping and quantum dense coding. Entanglement swapping is used as a fundamental building block in quantum relays and quantum repeaters for long distance communication. Quantum dense coding is a process of communication by sending two bits of classical information using only one qubit.

These processes are described here in realistic scenarios by taking into account imperfect sources of entangled photon pairs and detectors. Moreover, detectors used in quantum optical experiments occasionally produce dark counts and do not always detect incoming photons. These imperfections need to be taken into account when performing calculations involving detectors as in the cases of entanglement swapping and dense coding.

The conditional probabilities of different imperfect detectors and the state generated by two parametric down-conversion (PDC) sources after entanglement swapping are also discussed here. The four fold coincidence probability for entanglement swapping process including all imperfections is discussed in this dissertation. Furthermore, we modeled realistically the experimental dense coding process up to some extent. In this case we calculated the quantum state produced by a single realistic PDC source. We also calculated the probability to detect this state at the detectors in the case of ideal detection. The effect of nonlinearity of PDC crystal on this probability is also discussed here.

# Acknowledgement

I have no words to thank Allah Almighty for His uncountable blessing upon me and for giving me the strength and health to do this work.

I am very grateful to Dr. Aeysha Khalique, my M.phil supervisor, for introducing me to this subject and taught me how to do research. She always encouraged me to do independent research. She remained so cooperative during my work and always gave me very useful suggestions.

I also want to thank Prof. Asghar Qadir who always encouraged me to discuss any problem related to my work. I would also like to thank him, as DG NUST-CAMP and later Principal NUST-CAMP, for building this institution and providing an exemplary research environment for the students.

I wish to express my sincere gratitude to Prof. Muneer Ahmad Rasheed for his guidance and fruitful discussion during my research work.

I am also very much thankful to some of my senior colleagues specially Mr. Yasir Ali and Dr. Naseer Asif who were always there for me whenever I needed. Without their guidance and suggestions, it would have been difficult for me to get through this work.

Last but not least I wish to thank all my teachers, batch fellows, and staff members of CAMP.

# Contents

<b>1</b>	<b>Introduction</b>	<b>1</b>
<b>2</b>	<b>Modeling Imperfect Devices</b>	<b>10</b>
2.1	Introduction . . . . .	10
2.2	Lasers . . . . .	10
2.3	Single-Photon Sources . . . . .	11
2.4	Spontaneous Parametric Down-Conversion . . . . .	13
2.4.1	Type-I Down-Conversion . . . . .	14
2.4.2	Type-II Down-Conversion . . . . .	14
2.5	Modeling Imperfect Source . . . . .	15
2.5.1	Model of Imperfect Source for Entanglement Swapping . . . . .	17
2.5.2	Model of Imperfect Source for Dense Coding . . . . .	19
2.6	Quantum Mechanics of Beam Splitters . . . . .	19
2.7	Bell State Measurement . . . . .	24
2.8	Detector Model . . . . .	28
2.8.1	Ideal Photon-number Discriminating Detectors . . . . .	28
2.8.2	Inefficient Photon-number Discriminating Detectors with no Dark Counts . . . . .	29
2.8.3	Inefficient Photon-number Discriminating Detectors with Dark Counts . . . . .	30
2.8.4	Inefficient Threshold Detectors with Dark Counts . . . . .	35
<b>3</b>	<b>Realistic Entanglement Swapping</b>	<b>37</b>
3.1	Introduction . . . . .	37

3.2	Theoretical Entanglement Swapping . . . . .	38
3.3	Realistic Entanglement Swapping . . . . .	39
3.4	Comparison with Experimental Swapping . . . . .	44
<b>4</b>	<b>Theoretical Model for Exp. Dense Coding</b>	<b>52</b>
4.1	Introduction . . . . .	52
4.2	Quantum Dense Coding . . . . .	53
4.3	Theoretical Model of Quantum Dense Coding . . . . .	55
<b>5</b>	<b>Conclusion</b>	<b>65</b>
5.1	Sources and Detectors . . . . .	65
5.2	Theoretical Entanglement Swapping . . . . .	66
5.3	Theoretical Dense Coding . . . . .	66
	<b>References</b>	<b>68</b>

# Chapter 1

## Introduction

Early in the twentieth century physicists start to understand the behaviour of matter below the atomic level. The first and the foremost task is always measurement centred on the smallest quantity of matter that could be identified: the “quanta”-hence “ quantum” physics and later “qubit” in “quantum” information. Information science is the remarkable addition of that century. Quantum information and computation is the study of information processing tasks that can be achieved using quantum mechanical systems. Like many other simple and intense ideas, it was long ago that somebody thought of doing quantum information processing. To see why this is the case, we will have to go back in history to look at each of the fields which has contributed fundamental ideas to quantum mechanics, quantum information, quantum computation, computer science, information theory and cryptography. To get some feel of these different but essential perspectives which have come together in quantum information and computation, one should think oneself as the scientist of each of the fields described above. It is now expected that quantum information will play a revolutionary role in the next era of communication science. However, it is still a great challenge to the physicists and engineers to develop the methods for making large scale quantum information processing techniques.

Entanglement is a term used in quantum theory to describe the way that particles of energy/matter can become correlated to predictably interact with each other regardless of how far apart they are. To understand quantum entanglement, differ-



ent ideas and words must be explained, especially the idea of photons. The photon is a key concept in physics, and entanglement has the similar importance in quantum information processing that's why there is need to understand their behavior completely. When a photon (usually polarized laser light) passes through matter, it will be absorbed by an electron. Eventually after emitting photon electron will come back to its ground state . Certain crystal structures increase the probability that the photon will split into two photons of longer wavelengths than the original one. Moreover we know that longer wavelength means lower frequency and thus less energy. When the incident photon splits into two photons, the resulting photon pair is considered entangled.

*The process of using crystals to split incoming photons into pairs of photons is usually called parametric down-conversion.(see sec.2.4)*

Normally one of the split photons is aligned in a horizontal polarized cone and the other in a vertically polarized cone. By adjusting the experimental equipment these two cones can be made to overlap. Even though the polarization of the original incident photon is not known, quantum mechanics predicts they differ. In quantum information the simplest possible example of entangled states are Bell states. These are defined as a maximally entangled states of two qubits. An EPR pair is a pair of qubits which jointly are in Bell states, that is, entangled with each other. The four maximally entangled Bell states of a polarization entangled qubits can be written as,

$$|\phi^\pm\rangle = \frac{|H\rangle_A \otimes |H\rangle_B \pm |V\rangle_A \otimes |V\rangle_B}{\sqrt{2}}, \quad (1.0.1)$$

$$|\psi^\pm\rangle = \frac{|H\rangle_A \otimes |V\rangle_B \pm |V\rangle_A \otimes |H\rangle_B}{\sqrt{2}}. \quad (1.0.2)$$

Equation (1.0.1) illustrates that if the first party, let us say  $A$ , measures the qubit the outcome will be perfectly random either  $|H_A\rangle$  or  $|V_A\rangle$ ; either possibility having probability  $1/2$  where  $H$  and  $V$  represents the horizontal and vertical polarizations, respectively, of the photons while the subscripts  $A$  and  $B$  represents two parties. But if the second party, let us say  $B$ , measures the qubit, the outcome will be the same. Although the outcomes seem random, they are correlated. So far there is

nothing special: perhaps the two particles agreed in advance. To illustrate the state in Eq.(1.0.2), if an entangled photon strikes at a vertically polarized filter it may or may not pass through it. If it does, then its entangled partner will not, because the instant when the polarization of first photon is known, the second photon's polarization will known to be exactly opposite. It is the instant communication between the entangled photons to indicate each other's polarization that lies at the heart of quantum entanglement.

Entanglement is the most counter intuitive-feature of the quantum mechanics. It is at the heart of EPR paradox, of Bell's inequalities, and of the discussions of the nonlocality of quantum mechanics. Quantum theory is nonlocal in the sense that it predicts the correlations between the measurement outcomes that cannot be explained by the theories based completely on local variables. This prediction is confirmed by many experiments using pairs of entangled photons generated by a common source [1] or by having two particles interact with each other [2]. Also in 1993 Zukowski and colleagues [3] noticed that a common source is not necessary: nonlocality can exhibit itself also when the measurements are carried out on particles that have no common past ever, but have been entangled via the process of entanglement swapping. This alternative method to obtain entanglement is to make use of a projection of the state of the two particles onto an entangled state. A direct interaction between the particles is not necessary for this projection measurement.

Entanglement swapping processes given in Fig.(1.1) and Fig.(1.2) consist of two independent sources each generating a pair of particles and subject one particle from each pair  $B$  and  $C$  to an appropriate measurement, called Bell measurement which will be discussed in subsequent chapters in detail. This measurement projects the remaining two particles  $A$  and  $D$  which are totally independent of each other, onto an entangled state that may exhibit nonlocal correlations. This striking application of the projection postulate is referred to as entanglement swapping.

Entanglement swapping plays an important role in the context of quantum information science. For instance, it is the building block of protocols like quantum repeaters or quantum relays [3] proposed to increase the maximal distance in quantum communication. The first experimental demonstration of entanglement swapping

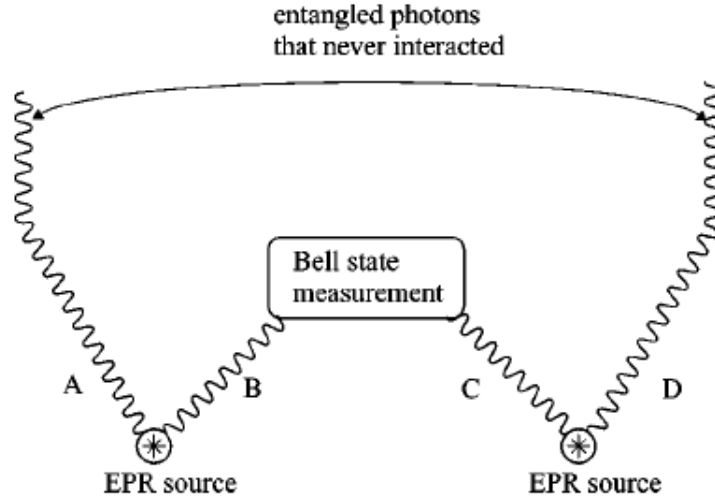


Figure 1.1: Scheme of principle of entanglement swapping.

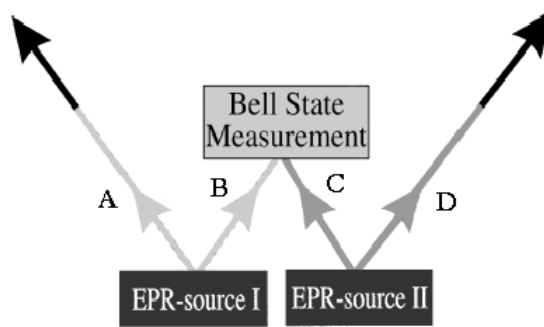


Figure 1.2: Principle of entanglement swapping. Two EPR sources produce two pairs of entangled photons, pair  $A-B$  and pair  $C-D$ . One photon from each pair (photons  $B$  and  $C$ ) is subjected to a Bell-state measurement. This results in projecting the other two outgoing photons  $A$  and  $D$  onto an entangled state. Change of the shading of the lines indicates the change in the set of possible predictions that can be made.

was reported in 1998, using two pairs of a polarization qubits encoded in photons around 800 nm created by two different parametric down-conversion (PDC) events in the same nonlinear crystal [4]. More recently (2002), an experiment with entangled qubits in Fock basis has been performed [5]. It involves only two photons instead of four. All the experiments conducted so far have demonstrated the entanglement swapping effect over short distances (of the order of meters). However, most processes in quantum information require this swapping effect to occur over large distances.

Two other forms of quantum information transmissions that have no classical

counterpart however, closely related to each other, are quantum teleportation [6] and quantum dense coding [7]. The first stage in these processes is that in which an entangled state (often called an Einstein-Podolsky-Rosen or EPR pair) is shared between two parties followed by a second stage in which this shared entangled state is used to achieve, transmission of a qubit via two classical bits and transmission of information of two classical bits by sending only one qubit, respectively. Thus quantum dense coding provides a method by which the classical information of two bits can be transmitted by communicating only one qubit of quantum information. Entanglement by itself cannot be used to transmit a classical data, however it can reduce the amount of classical communication required to perform a distributed computation [3]. The latter refers to the amount of communication required to evaluate a function of several inputs in remote locations. For example, if both Alice and Bob have separate appointment calendars with  $n$ -time slots, then  $O(n)$  bits of information are required to determine if there is a time when both are free. However, if they are allowed to share prior entanglement, or if they are allowed to communicate using quantum bits (qubits) rather than the bits, the communication complexity is reduced to  $O(\sqrt{n} \log n)$  [8].

The dense coding protocol is based on a counter-intuitive idea of instant communication or transmission of information through quantum correlations between entangled states. The theoretical model of quantum dense coding is given in sec.4.2. The concept of dense coding was noted by EPR in 1935, but was ignored in practice until the development of the theory of quantum computing and quantum information in the early 90's; when many researchers all around the world got into experimentally showing the validity of the phenomena predicted by the theory of EPR pairs. Now when entanglement entered in to quantum theory, the EPR article became a hindrance for quantum theoreticians. But through Bell's inequalities it has been shown that randomness is inherent in the quantum description of reality [9]. This effect has been shown even further with experimental breakthroughs in quantum computing protocols, including the dense coding protocol.

The proposal of the dense coding protocol making use of the properties of entangled particles revived research in quantum information and quantum computing

around the world. In their paper on quantum communication using EPR pairs Bennett and Wiesner [6], have shown that the maximally entangled Bell states are ideal for quantum communication methods, particularly in quantum dense coding. In that article they described the dense coding process theoretically, and also proposed that it would be extremely difficult to achieve this task through spin entangled states. However, they also proposed experimental dense coding using a polarized entangled photons and parametric down-conversion in crystals.

The earlier mentioned processes i.e superdense coding and teleportation have received a lot of experimental attention recently. In this context the first experimental realization of dense coding was achieved by Mattle et al [10]. They used degenerate noncollinear type-II down-conversion in nonlinear BBO (Beta-Barium-Borate) crystals to generate polarization entangled photon pairs. The two parties, Alice and Bob, share that entangled pair and Bob communicates with Alice by sending her some information through polarization encoding. For this purpose, the necessary transformation of Bob's particle was attained by using a half-wave retardation plate for changing the polarization (i.e from  $H \rightarrow V$  or  $V \rightarrow H$ ) and quarter wave-plate to generate the polarization phase shift <sup>1</sup>. This encoded beam was then combined with the other beam at Alice's Bell-state-analyzer. Two channel polarizers are placed in each of its out ports and proper coincidence analysis between four single-photon detectors. Using such kind of configuration, one can distinguish the Bell states due to different outcomes of the interference at the beam splitter. Thus, two bits of information can be sent via Bob's two state particle to Alice, who finally gets the encoded information by determining the Bell state of the entangled two state particle system.

The experimental realization of quantum processes has never been an easy task for experimentalists. There occur different kinds of limitations to perform quantum processes practically and to construct physical networks. We are going to discuss the difficulties that occur in the field of quantum communication especially in entan-

---

<sup>1</sup>The component polarized along the axis of the quarter-wave plate is advanced only by  $\frac{\pi}{2}$  relative to the other. Reorienting the optical axis from vertical to horizontal causes a net phase change of  $\pi$  between  $|H\rangle$  and  $|V\rangle$ .

lement swapping and quantum dense coding. One of these problems was to have a perfect source that can generate an ideal single-photon. A single-photon source can be created by such a pair just by detecting one photon of the pair, and then knowing that its partner was created at the same time. In 1991, Ekert proposed a method of secure communication by considering a source that emits a pair of spin half particles in a singlet state [11]. These two particles fly off to two distant parties who need to communicate with each other, where they are detected by analyzers aligned randomly in either of two orthogonal basis. In 1970, Burnham and Weinberg [12] demonstrated spontaneous parametric down-conversion (SPDC) to create an entangled photon pair. In parametric down-conversion an entangled photon pair is created by pumping a laser field into a nonlinear crystal [13]. Photons passing through the crystal can decay into a pair of identical or non-identical photons. Multi-photon pair source was also considered when analyzing entanglement swapping. When multi-photon events occur it is possible that one of the two photons involved in the swap is actually from a different pair and the entanglement required for a successful swap is absent altogether. However, this type of occurrence leads to error in swapping process and limits the fidelity of an extended swapping operation. All methods currently available for generating photon pairs cannot create a perfect single-photon but there occur multipair sources as well which cause the error in perfect communication.

Quantum networking becomes much more difficult when we talk about long distance transmissions. For long distance quantum communication employing quantum repeaters [14] or relays [3], it is particularly important to examine the effect of how entangled states after entanglement swapping are affected by the experimental imperfections. Collins et al. [3] studied the impact of transmission losses and detectors noise as well as dark counts (i.e detector clicks even if there is no photon) on the performance of quantum relays. Brask and Sorensen have studied the effect of multi excitation events in PDC in addition to imperfect detectors and transmission losses on quantum repeater performance has been examined perturbatively [3]. Imperfect detectors are among the main hurdles in implementing quantum communication networks. These imperfections include noise of the detectors and dark counts which

reduce the efficiency of receiving data. Modern technology has not been able to make perfect detectors as yet. Photons can transfer information at the speed of light through a free space or down a fibre optic cable, but they are easily absorbed during collisions and lost along the way. This is what we call channel losses or transmission losses, however this loss of photons during transmission can easily be accounted for with a factor on the transmission success probability

$$t = 10^{\frac{-l\beta}{10}}, \quad (1.0.3)$$

where  $t$  is the transmission coefficient or probability of successful transmission,  $l$  is the distance traveled and  $\beta$  is the loss coefficient of transmission medium in units of  $d_B$  [3]. The probability of photon detection at some detector becomes smaller than the probability of dark counts at that detector for distances larger than 100km. At that point it is no longer possible to communicate, as signal to noise ratio becomes too small. Thus, such limitations together with channel losses are the main factors of insecure less efficient quantum communication in physical world over long distances.

Experimental realization of such quantum processes has gained importance because of their implementations in real world. Theoretical understanding of these processes has become enormously important to design physical networks. The main motivation behind this dissertation is to give a realistic scheme for entanglement swapping and quantum dense coding discussing practical limitations which could be useful to pre-analyze the efficiency of quantum communication over long distances. These limitations include all kind of imperfections which reduce the efficiency of these quantum processes. The reviewed work, is mostly based on entanglement swapping. In chapter 2, imperfect devices are modeled where generation of single-photon pairs, probability of imperfect detectors to detect these photons and transmission losses are discussed in detail. In chapter 3, the state after entanglement swapping is analyzed by including such imperfections and then the probability with which the state occurs is calculated. A theoretical model of quantum dense coding in experimental communication including these practical limitations is discussed in chapter 4 and to my knowledge this is not attempted before. This theoretical model is based on the experimental model of quantum dense coding presented by Mattle et al. in [10] in

which entangled photon pair is generated by degenerate noncollinear type-II PDC in antisymmetric state  $|\psi^-\rangle$ . The fourfold coincidence probability to detect this state at the detectors is also calculated by considering imperfections in this model.



# Chapter 2

## Modeling Imperfect Devices

### 2.1 Introduction

Application of quantum communication such as quantum cryptography, quantum teleportation, quantum relays and linear optics quantum computing [3] use entangled photon pair sources. In addition entangled photon pair sources are essential for different application of modern information technology. Most applications require very bright, efficient and well controlled sources of entanglement, which means they should be well coupled into optical fibers and equally be well adapted to free space optics. Experimental realization is very different from the theoretical realization of quantum information processes due to imperfect entangled photon pair sources and detectors. Here, first I will describe some experimental sources which are being used to produce entangled photons and single-photon as well these days and then I will explain the model of imperfect sources and detectors which are being used for entanglement swapping and dense coding experiments. The model being used is the same as that in entanglement swapping experiment in [3, 15].

### 2.2 Lasers

Lasers are the most practical and the most efficient light sources to produce entangled photons which are used these days. For this reason the majority of the groups working in the field of quantum optics use these sources. I will not go into the

detailed discussion of these sources later and here present a brief review of them. The light generated by laser in a given mode is described by a coherent state of the field [16].

$$|\sqrt{\mu}e^{i\theta}\rangle \equiv |\alpha\rangle = e^{-\frac{\mu}{2}} \sum_{n=0}^{\infty} \frac{\alpha^n}{\sqrt{n!}} |n\rangle, \quad (2.2.1)$$

where  $\mu = |\alpha|^2$  is the average photon number. The phase factor  $e^{i\theta}$  is only accessible when reference for the phase is available if not, then the emitted state is rather described by the mixture

$$\rho = \int_0^{2\pi} \frac{d\theta}{2\pi} |\alpha\rangle\langle\alpha| \quad (2.2.2)$$

$$= \sum_{n=0}^{\infty} \text{Pr}(n|\mu) |n\rangle\langle n|, \quad (2.2.3)$$

with conditional probability

$$\text{Pr}(n | \mu) = e^{-\mu} \frac{\mu^n}{n!}. \quad (2.2.4)$$

The randomization of phase generalizes to a multimode coherent states. Since any two equivalent decompositions of the same density matrix are indistinguishable so one can say that in the absence of a phase reference, the laser produces a *Poissonian* mixture of number states.

## 2.3 Single-Photon Sources

A laser source randomly generates photons, so even using an attenuated laser has at least some chance that there may be more than one photon between the source and the detector. So the source of antibunched photons is required to get as close as possible to having a single-photon between the source and the detector. Photon exhibit generally refers to a light field with photons more equally spaced than a coherent laser field [17] and a signal at detectors is anticorrelated. More specifically, it can refer to *sub-Poisson* photon statistics, that is a photon number distribution for which the variance is less than the mean. This requires a source consisting of very few atoms, ideally a single atom. Such sources were developed only relatively recently by Grangier et al [18]. This kind of sources consist of a beam of calcium irradiated

by laser light to a higher energy S-state. This state then rapidly decays to a P-state by emitting a photon of frequency  $\nu_1$ . Subsequently the atom rapidly undergoes another decay to a ground S-state by emitting a second photon of frequency  $\nu_2$  as shown in figure(2.1).

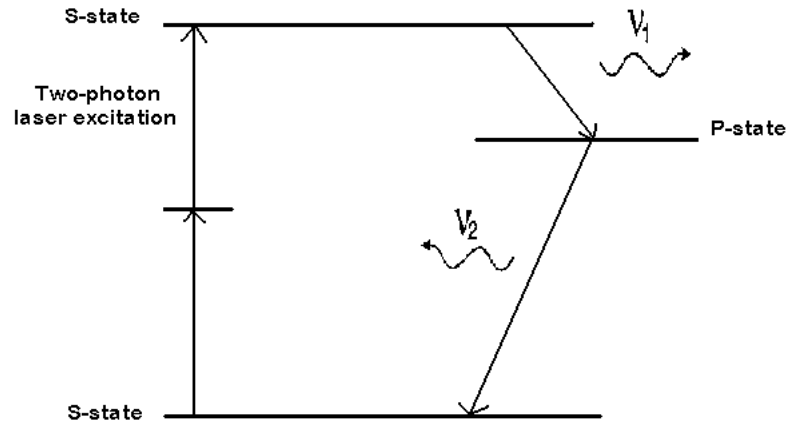


Figure 2.1: Energy level diagram of a calcium atom irradiated by laser acting as single-photon source for the experiments Grangier et al.

In the experiment described in [18], the first photon is detected by the detector  $D_{trig}$ , was used to alert the set of other photo-detectors placed at the output ports of the 50 : 50 beam splitter on which the second photons falls as shown in Fig.(2.2).

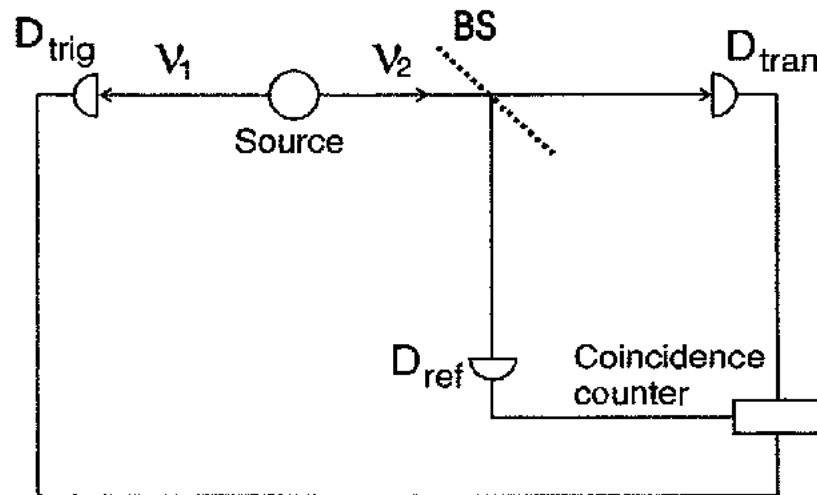


Figure 2.2: Anti correlation experiment of Grangier et al.

This trigger tells the detectors to expect a photon to emerge from the beam

splitter by “gating” the detection electronics for a brief time interval. This eliminates the irrelevant counts due to the photons from irrelevant sources (e.g environment). The experimental set up shown in Fig.(2.2) allows only a single-photon to fall on the detectors. This photon would be either reflected into the detector  $D_{ref}$  or transmitted into the detector  $D_{tran}$  i.e it is “which path” experiment and no interference will occur. The counts should be anti-correlated and no simultaneous counts of the transmitted and reflected photons. As the beam splitter is 50 : 50, so the repetition of the experiment should result in each of the two detectors firing approximately 50 percent. These expectations are confirmed by the investigators.

## 2.4 Spontaneous Parametric Down-Conversion

Entanglement between the photons cannot be created by coupling via an interaction yet. However, there are several processes, such as atomic cascade decays or parametric down-conversion, where, the properties of two emitted photons become entangled. Historically, entanglement was first observed between spatially separated quanta during the process of measurements of polarization correlation between  $\gamma^+\gamma^-$  in positron annihilation [19]. Soon after Bohm’s proposal for observing EPR phenomena in spin half systems and Bell’s discovery that contradictory predictions between quantum theories can actually be observed, a series of experiments was performed, mostly using a polarization entangled photons from a two photon cascade emission from calcium [19]. From these experiments, it was found that the two photons were in the visible region, and could be controlled by using standard optical techniques. This is a great advantage in comparison to the positron annihilation source; however, the two emitted photons are no longer in the opposite directions to conserve momentum, since the emitted atom carries away some randomly determined momentum. This reduces the brightness of the source and makes experimentally difficult to handle. The process of parametric down-conversion(PDC) is more efficient to produce entangled photon pair being used these days [19].

Spontaneous parametric down-conversion (SPDC) is an important process in quantum optics to produce entangled photons. When photons strike the nonlinear

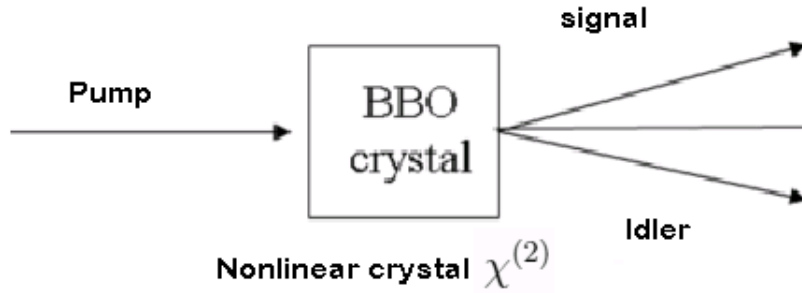


Figure 2.3: Spontaneous parametric down-conversion.

crystal e.g BBO (Beta-Barium Borate) crystal [20], they split up into two photons of lower energy and momentum. The conservation of energy gives rise to entanglement in various degrees of freedom such as position and momentum, time and energy. The state of the crystal is left unchanged and this leads to the phase matching in nonlinear optics. In SPDC, the photon pairs are created at random times. However, the detection of one of the pair (the signal) confirms the presence of its partner (the idler). On the basis of output of this process, the SPDC is divided into two kinds.

### 2.4.1 Type-I Down-Conversion

In type-I down-conversion signal and idler share the same polarization direction. For example, the pump has the extraordinary polarization but the idler and signal both possess the ordinary polarization. Different colours are separated into cones centered on the pump beam. The outcome of type-I down-conversion is squeezed vacuum that contains even number photon terms.

### 2.4.2 Type-II Down-Conversion

In type-II down-conversion the outgoing photons have perpendicular polarization. In this process, the pump has the extraordinary polarization. It means the division of light into two components “ordinary and extraordinary” found in material which has two different indices of refraction in two different directions such as *calcite*. When light enters, it splits into two beams which travel with different speeds in order to

fulfill the momentum conservation condition inside the crystal (phase matching). The two down converted photons have different, for most orthogonal polarizations, offering the possibility of a new source of polarization entanglement.

## 2.5 Modeling Imperfect Source

Now we will see how to model the imperfect source for quantum information processing. We will use these models throughout in our discussion on different quantum information processes and specifically on “realistic entanglement swapping and dense coding”. The ideal photon pair source would create exactly one entangled photon pair on demand. Such sources do not exist yet. Realistic or imperfect sources are probabilistic in nature. They generate photon pairs at random instances within those time intervals allowed by pump laser and sometimes emitting two or even more photon pairs. In PDC the rate of pair generation is proportional to the nonlinearity  $\chi^{(2)}$ , the strength of the pump field and, the interaction time.

Many active and passive (i.e photon number conservation) optical transformation can be described by using basic  $SU(1, 1)$  and  $SU(2)$  Lie algebra respectively. The parametric down-conversion are active transformations as they create or annihilate photon pairs. The Lie algebra  $SU(1, 1)$  has been shown in [21, 22] to describe these transformations. The set of operators  $\{M_x, M_y, M_z\}$  provides a basis for  $SU(1, 1)$  algebra with the commutation relations,

$$[M_x, M_y] = -iM_z, \quad [M_y, M_z] = iM_x, \quad [M_z, M_x] = iM_y. \quad (2.5.1)$$

Appropriate  $SU(1, 1)$  realization for degenerate PDC (i.e two photons in pair are identical) are one-boson realizations given by the generators

$$\begin{aligned} M_x^{(i)} &= \frac{1}{4}(\hat{c}_i^\dagger \hat{c}_i^\dagger + \hat{c}_i \hat{c}_i), \\ M_y^{(i)} &= \frac{1}{4i}(\hat{c}_i^\dagger \hat{c}_i^\dagger - \hat{c}_i \hat{c}_i), \\ M_z^{(i)} &= \frac{1}{4}(\hat{c}_i^\dagger \hat{c}_i + \hat{c}_i \hat{c}_i^\dagger). \end{aligned} \quad (2.5.2)$$

Here the annihilation operator  $\hat{c}_i$  refers to any of  $\hat{a}_+, \hat{a}_-, \hat{b}_+, \hat{b}_-$ .

For nondegenerate PDC (i.e two nonidentical photons in pair), the appropriate realizations of  $SU(1, 1)$  are two-boson realizations given by the generators

$$\begin{aligned} M_x^{(ij)} &= \frac{1}{2}(\hat{c}_i^\dagger \hat{c}_j^\dagger + \hat{c}_i \hat{c}_j), \\ M_y^{(ij)} &= \frac{1}{2i}(\hat{c}_i^\dagger \hat{c}_j^\dagger - \hat{c}_i \hat{c}_j), \\ M_z^{(ij)} &= \frac{1}{4}(\hat{c}_i^\dagger \hat{c}_i - \hat{c}_j \hat{c}_j^\dagger). \end{aligned} \quad (2.5.3)$$

For type-I PDC, where photons are created in the same polarization, typically  $\hat{c}_i = \hat{a}_+$  and  $\hat{c}_j = \hat{b}_+$ , whereas in type-II PDC with opposite polarizations of photons,  $\hat{c}_i = \hat{a}_+$  and  $\hat{c}_j = \hat{b}_-$ . The generation of entangled photon pairs is possible using type-II PDC, where the emission directions of  $a$  and  $b$  photons are made to overlap. A PDC process can be described and represented mathematically by one parameter  $SU(1, 1)$  transformation of the vacuum state [3],

$$Y(\gamma) | vac \rangle = \exp(i\gamma K_x) | vac \rangle \quad \gamma \in R. \quad (2.5.4)$$

Here,  $K_x$  is one of the generators of  $SU(1,1)$  group ( $K_x, K_y, K_z$ ) and defined by these commutation relations,

$$[K_x, K_y] = -iK_z, \quad [K_y, K_z] = iK_x, \quad [K_z, K_x] = iK_y. \quad (2.5.5)$$

Let us consider for example the type-I nondegenerate (non identical photons) PDC, in which the photon pairs are created in the same polarization, the generator for this case is given by the the following two-boson realization,

$$K_x = \frac{1}{2}(a_v^\dagger b_v^\dagger + \hat{a}_v \hat{b}_v), \quad (2.5.6)$$

where,  $\hat{a}_v$  and  $\hat{b}_v$  are the creation and annihilation operators corresponding to the vertical polarization of two different modes  $a$  and  $b$ .

Now in the case of realistic sources, the resultant generated quantum state is not just a pair of photons but the superposition of photon number states. It also includes the vacuum and pairs-of-pairs and even higher order terms. For small values of  $\gamma$  the state given in Eq.(2.5.4) can be approximated as

$$Y(\gamma) | vac \rangle = | vac \rangle + \frac{i\gamma}{2} | 0110 \rangle, \quad (2.5.7)$$

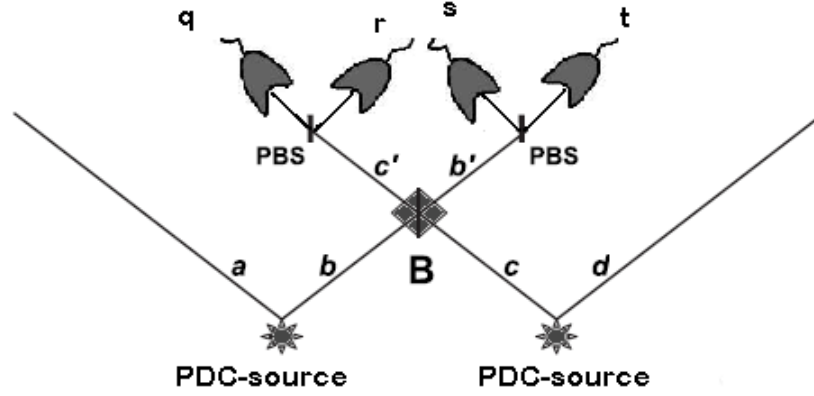


Figure 2.4: Entanglement swapping of photon-polarization qubits based on two PDC sources and a Bell-state measurement with four imperfect photon detectors. Four spatial modes are involved, labeled by  $a, b, c,$  and  $d$ . Two modes, one from the first and one from the second source,  $b$  and  $c$ , respectively, are combined at a balanced beam splitter ( $B$ ). The exits of the latter, denoted by  $b'$  and  $c'$ , respectively, are directed to polarizing beam splitters (PBSs) and then detected at four detectors: one for the H and one for the V polarization of each of the  $c'$  and  $b'$  modes. The four detectors are inefficient photon detectors subject to dark counts. Their readout is denoted by  $(qrst)$ . Given this readout we are interested in the entangled quantum state of the remaining  $a$  and  $d$  modes depending on experimental parameters characterizing the deficiencies of the experiment.

where, the Fock notation  $|ijkl\rangle$  of the state represents a state with  $i, j, k, l$  photons in  $a_h, a_v, b_v, b_h$  modes respectively. We have chosen the order HVVH. The strong vacuum component in Eq.(2.5.7) implies that when pump laser beam is sent, it will either lead to the down-conversion or not. That means there is a high probability that PDC will not take place at all.

### 2.5.1 Model of Imperfect Source for Entanglement Swapping

Two PDC sources are required for swapping experiment as shown in Fig.(2.4). Each of the two sources emit two polarization entangled photon pairs which are labeled as  $a, b$  and  $c, d$ . These photons have mutually exclusive polarizations which are labeled as H and V corresponding to horizontal and vertical polarizations. Here we are assuming a type-I nondegenerate PDC for both sources. The experimental setup can be realized by using a pair of identical crystals stacked together such that their axes are orthogonal to each other and the pump laser is diagonally polarized. Such a combination of two crystals effectively creates a PDC producing two-mode squeezed states of the form given in Eq.(2.5.4). The complete quantum state prepared by



these two sources is then mathematically represented as

$$\begin{aligned} |\chi\rangle &= \exp[i\chi(\hat{a}_H^\dagger \hat{b}_H^\dagger + \hat{a}_H \hat{b}_H)] \otimes \exp[i\chi(\hat{a}_V^\dagger \hat{b}_V^\dagger + \hat{a}_V \hat{b}_V)] \otimes \exp[i\chi(\hat{c}_H^\dagger \hat{d}_H^\dagger + \hat{c}_H \hat{d}_H)] \\ &\otimes \exp[i\chi(\hat{c}_V^\dagger \hat{d}_V^\dagger + \hat{c}_V \hat{d}_V)] |vac\rangle. \end{aligned} \quad (2.5.8)$$

The generated quantum state is parameterized by  $\chi = \frac{\gamma}{2} \in R$ . Here we will consider  $\chi$  as the efficiency of the source and also assume that both the sources have same efficiency for entanglement swapping. It is convenient to express Eq.(2.5.8) in normal ordered form [3], given two independent bosonic modes  $a$  and  $b$ , we are choosing a different basis in Eq.(2.5.5) in order to obtain a two mode bosonic representation of  $SU(1,1)$  Lie algebra,

$$\hat{K}_+ = \hat{a}^\dagger \hat{b}^\dagger, \quad \hat{K}_- = \hat{a} \hat{b}, \quad \hat{K}_0 = \frac{1}{2}(\hat{a}^\dagger \hat{a} + \hat{b}^\dagger \hat{b} + 1). \quad (2.5.9)$$

These new generators form the basis  $\{\hat{K}_0, \hat{K}_-, \hat{K}_+\}$  of  $SU(1,1)$  Lie algebra which satisfies the following commutation relations:

$$[\hat{K}_-, \hat{K}_+] = 2\hat{K}_0, \quad [\hat{K}_0, \hat{K}_\pm] = \pm \hat{K}_\pm. \quad (2.5.10)$$

The normal-ordered decomposition formula holds for the generators of  $SU(1,1)$  Lie algebra is according to [3],

$$\exp[\alpha_+ \hat{K}_+ + \alpha_0 \hat{K}_0 + \alpha_- \hat{K}_-] = \exp[A_+ \hat{K}_+] \exp[\ln(A_0) \hat{K}_0] \exp[A_- \hat{K}_-], \quad (2.5.11)$$

where,  $A_0, A_\pm$  are given as

$$A_\pm = \frac{(\alpha_\pm) \sinh \theta}{\cosh \theta - (\frac{\alpha_0}{2\theta}) \sinh \theta}, \quad (2.5.12)$$

$$A_0 = [\cosh \theta - (\frac{\alpha_0}{2\theta}) \sinh \theta], \quad (2.5.13)$$

$$\theta = [(\frac{\alpha_0}{2})^2 - \alpha_+ \alpha_-]^{1/2}. \quad (2.5.14)$$

Thus using these decomposition rule transformations the following special case is derived which is required here:

$$\exp[i\chi(\hat{a}^\dagger \hat{b}^\dagger + \hat{a} \hat{b})] = \exp[\phi(\chi) \hat{a}^\dagger \hat{b}^\dagger] \exp[\omega(\chi)(\hat{a}^\dagger \hat{a} + \hat{b}^\dagger \hat{b} + 1)] \exp[\phi(\chi) \hat{a} \hat{b}], \quad (2.5.15)$$

where the following definition is introduced

$$\phi(\chi) := i \tanh \chi, \quad (2.5.16)$$

$$\omega(\chi) := -\ln[\cosh \chi], \quad (2.5.17)$$

each of the factors in Eq.(2.5.8) can be decomposed in this way. By doing so and using the fact that annihilation and creation operators corresponding to different optical modes commute, we get this equation

$$\begin{aligned} |\chi\rangle &= \exp[4\omega(\chi)] \exp[a_H^\dagger b_H^\dagger + a_V^\dagger b_V^\dagger + c_H^\dagger d_H^\dagger + c_V^\dagger d_V^\dagger] \\ &\times \exp[\omega(\chi)(a_H^\dagger a_H + a_V^\dagger a_V + b_H^\dagger b_H + b_V^\dagger b_V + c_H^\dagger c_H + c_V^\dagger c_V + d_H^\dagger d_H + d_V^\dagger d_V)] \\ &\times \exp[\phi(\chi)(a_H^\dagger b_H + a_V^\dagger b_V + c_H^\dagger d_H + c_V^\dagger d_V)]|vac\rangle. \end{aligned} \quad (2.5.18)$$

The last two exponential factors leave the vacuum state unchanged and the final form of above equation will be

$$|\chi\rangle = \exp[4\omega(\chi)] \exp[\phi(\chi)(a_H^\dagger b_H^\dagger + a_V^\dagger b_V^\dagger + c_H^\dagger d_H^\dagger + c_V^\dagger d_V^\dagger)]|vac\rangle. \quad (2.5.19)$$

This is the required normal-ordered form of the quantum state generated by the two PDC sources.

## 2.5.2 Model of Imperfect Source for Dense Coding

For dense coding the model is relatively simple as only one source is required for this process. The state generated by degenerate type-II PDC can be calculated by using  $SU(1, 1)$  Lie algebra for type-II PDC, where the generator for two-boson realization is given by Eq.(2.5.4) taking  $\hat{c}_i = \hat{a}_+$  and  $\hat{c}_j = \hat{b}_-$ . Therefore the generator for this case will become of the form

$$J_x = \frac{1}{2}(\hat{a}_h^\dagger \hat{b}_v^\dagger + \hat{a}_h \hat{b}_v). \quad (2.5.20)$$

Now using the above simple algebra given in section(2.5.1), the state generated by degenerate type-II parametric down-conversion is

$$|\chi\rangle = \exp[2\omega(\chi)] \exp[\phi(\chi)(\hat{a}_h^\dagger \hat{b}_v^\dagger - \hat{a}_v^\dagger \hat{b}_h^\dagger)]|vac\rangle. \quad (2.5.21)$$

## 2.6 Quantum Mechanics of Beam Splitters

A beam splitter is an interesting optical device that splits a beam of incoming light in two. It is a very important part of most interferometers. For “classical” light

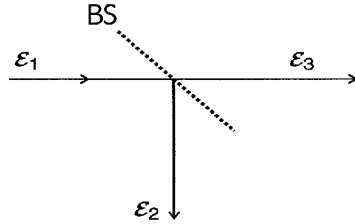


Figure 2.5: Classical beam splitting. A classical field of amplitude  $E_1$  is split into two field of amplitude  $E_2$  and  $E_3$ .

beams, coherent and thermal beams, the quantum and classical treatments the beam splitters agree [23] but the results go wrong and quite misleading in the case of a single or few photons.

Let us see first how the classical reasoning goes wrong. Let us consider a lossless beam splitter and a classical light field with a complex amplitude  $E_1$  incident on it as shown in Fig.(2.5). The reflected and the transmitted beams have amplitudes  $E_2$ ,  $E_3$  respectively. If  $r$  and  $t$  are the reflectance and transmittance of the beam splitter, then it follows that

$$E_2 = rE_1 \quad , \quad E_3 = tE_1. \quad (2.6.1)$$

The sum of intensities of the reflected and transmitted beams (output beams) should be equal to the intensity of the incident beam as we have assumed a lossless beam splitter.

$$|E_1|^2 = |E_2|^2 + |E_3|^2, \quad (2.6.2)$$

which requires that

$$|r|^2 + |t|^2 = 1. \quad (2.6.3)$$

Now for the quantum mechanical treatment of a lossless beam splitter, we try to use the same reasoning by replacing complex field amplitudes  $E_i$  by annihilation operators  $\hat{a}_i$  ( $i = 1, 2, 3$ ) as shown in Fig.(2.6).

$$\hat{a}_2 = r\hat{a}_1 \quad , \quad \hat{a}_3 = t\hat{a}_1. \quad (2.6.4)$$

However, the operators corresponding to the field are supposed to satisfy the

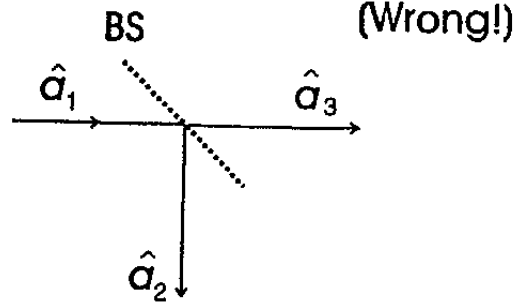


Figure 2.6: Incorrect quantum mechanical description of beam splitter.

commutation relations given below.

$$[\hat{a}_i, \hat{a}_j^\dagger] = \delta_{ij} \quad [\hat{a}_i, \hat{a}_j] = 0 = [\hat{a}_i^\dagger, \hat{a}_j^\dagger] \quad (i, j = 1, 2, 3). \quad (2.6.5)$$

But it is easily seen that for the operators in Eq.(2.6.4) we obtain

$$\begin{aligned} [\hat{a}_2, \hat{a}_2^\dagger] &= |r|^2 [\hat{a}_1, \hat{a}_1^\dagger] = |r|^2, \\ [\hat{a}_3, \hat{a}_3^\dagger] &= |t|^2 [\hat{a}_1, \hat{a}_1^\dagger] = |t|^2, \\ [\hat{a}_2, \hat{a}_3^\dagger] &= rt^* \neq 0 \text{ etc.} \end{aligned} \quad (2.6.6)$$

Thus we obtain the transformation given in Eq.(2.6.4) which does not preserve the commutation relations and therefore cannot give the correct quantum mechanical description of a beam splitter. The reason behind this failure is that in the classical picture there is an unused “port” of the beam splitter which, being empty of an input field and has no effect on the output beams. But, in quantum mechanical picture, this “unused” port still contains a quantized field mode albeit in the vacuum state which has strong contribution in the state generated from a PDC source. For a proper quantum mechanical description of the beam splitter, the required modes are shown in the Fig.(2.7) , where  $\hat{a}_0$  represents the vacant input mode of classical field operator. There are two other sets representing the transmittance and reflectance of the beam splitter. Now the beam splitter transformations of field operators can be written as

$$\hat{a}_2 = r\hat{a}_1 + t'\hat{a}_0, \quad \hat{a}_3 = t\hat{a}_1 + r'\hat{a}_0, \quad (2.6.7)$$

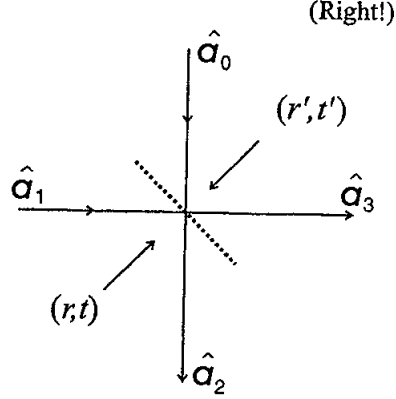


Figure 2.7: Correct quantum mechanical description of beam splitter.

or collectively as

$$\begin{pmatrix} \hat{a}_2 \\ \hat{a}_3 \end{pmatrix} = \begin{pmatrix} t' & r \\ r' & t \end{pmatrix} \begin{pmatrix} \hat{a}_0 \\ \hat{a}_1 \end{pmatrix}. \quad (2.6.8)$$

It can be easily seen that the commutation relations given in Eq.(2.6.5) are satisfied if the following relations hold,

$$|r'| = |r|, \quad |t'| = |t|, \quad |r|^2 + |t|^2 = 1, \quad r^*t' + r't^* = 0 \quad \text{and} \quad r^*t + r't'^* = 0. \quad (2.6.9)$$

When a light beam passes through the beam splitter it suffers a phase shift but this phase shift depends on the construction of the beam splitter [24]. For example if the beam splitter is constructed as a single dielectric layer, the reflected and the transmitted beams will differ by a phase factor of  $\exp(\pm i\frac{\pi}{2}) = \pm i$ . For a 50 : 50 beam splitter, let us assume that the reflected beam suffers a phase shift of  $\frac{\pi}{2}$ , then the input and output modes are related to each other through beam splitter as  $\begin{pmatrix} a_2 \\ a_3 \end{pmatrix} \rightarrow U \begin{pmatrix} a_0 \\ a_1 \end{pmatrix}$  where,

$$U = \frac{1}{\sqrt{2}} \begin{pmatrix} 1 & i \\ i & 1 \end{pmatrix},$$

$$\hat{a}_2 = \frac{1}{\sqrt{2}}(\hat{a}_0 + i\hat{a}_1), \quad \hat{a}_3 = \frac{1}{\sqrt{2}}(i\hat{a}_0 + \hat{a}_1). \quad (2.6.10)$$

This transformation is a Heisenberg picture formulation of beam splitter. Since the transformations between input and output modes should be unitary, so Eq.(2.6.8) can be written as

$$\begin{pmatrix} \hat{a}_2 \\ \hat{a}_3 \end{pmatrix} = \hat{U}^\dagger \begin{pmatrix} \hat{a}_0 \\ \hat{a}_1 \end{pmatrix} \hat{U}, \quad (2.6.11)$$

where for a specific transformation like Eq.(2.6.10), the unitary operator  $\hat{U}$  has the following form,

$$\hat{U} = \exp[i\frac{\pi}{4}(\hat{a}_0^\dagger\hat{a}_1 + \hat{a}_0\hat{a}_1^\dagger)]. \quad (2.6.12)$$

On the other hand, we can also adopt the Schrodinger picture formulation and can find the output state for a given input state to the beam splitter [23]. As we know that the photon number states, their superposition or any statistical mixture of such states can be constructed by the action of creation operators on the vacuum state.

If a single-photon is incident on any one of the input ports of the beam splitter, while the other port containing only vacuum, will be either transmitted or reflected with equal probability. Obviously the beam splitter is a passive device that means it neither creates nor destroys photons. One important aspect of beam splitter action is that it also creates the entanglement between the input states.

Now we return to the strictly quantum domain and consider the situation where single photons are simultaneously incident on the two input ports of 50 : 50 beam splitter, the incident state being  $|1\rangle_0|1\rangle_1 = \hat{a}_0^\dagger\hat{a}_1^\dagger|0\rangle|0\rangle$ . Again following the previous procedure with transformations  $\hat{a}_0^\dagger = (\hat{a}_2^\dagger + i\hat{a}_3^\dagger)/\sqrt{2}$  and  $\hat{a}_1^\dagger = (i\hat{a}_2^\dagger + \hat{a}_3^\dagger)/\sqrt{2}$  we have

$$\begin{aligned} |1\rangle_0|1\rangle_1 &\xrightarrow{BS} \frac{1}{2}(\hat{a}_2^\dagger + i\hat{a}_3^\dagger)(i\hat{a}_2^\dagger + \hat{a}_3^\dagger)|0\rangle_2|0\rangle_3 \\ &\xrightarrow{BS} \frac{i}{2}(\hat{a}_2^\dagger\hat{a}_2^\dagger + \hat{a}_3^\dagger\hat{a}_3^\dagger)|0\rangle_2|0\rangle_3 \end{aligned} \quad (2.6.13)$$

Apparently, the photon detectors placed at the output ports of the beam splitter should not register simultaneous counts when two photons emerge together. Physically this does not mean that photons do not exhibit a particle nature. Rather, it is caused due to interference between two possible ways of obtaining the (absent) output state  $|1\rangle_2|1\rangle_3$ .

## 2.7 Bell State Measurement

Bell state measurement projects the state of a two level system onto the complete set of orthogonal maximally entangled Bell states. Bell states are key element of the most of the quantum information processes. This provides a quantum correlation which can be used in certain important processes such as teleportation [7], quantum dense coding [6] and entanglement swapping [3] which allow the entanglement between the two particles that were totally independent in the past. The problem of creating Bell states has been resolved by using parametric down-conversion (PDC) in non linear crystals.

The transformation of an entangled state to an unentangled state is the main ingredient of the Bell state analysis. The necessary coupling has not yet been achieved for photons. But it turns out that interference of two entangled particles, and thus the photon statistics behind the beam splitter depends on the entangled state that the pair is in [19].

Let us first consider the generic case of two interfering particles. If there are two otherwise indistinguishable particles in two different beams and these two beams overlap at the beam splitter, we can ask the question, what will be the probability of finding the two particles in different output ports of the beam splitter. Alternatively we can ask, what is the probability that two detectors, one in each output beam, detect one photon each.

With any beam splitter, at the best two of the four Bell-states can be identified with certainty. To detect polarization entangled states, two photons  $a$  and  $b$  are brought to interference at a 50 : 50 beam splitter as illustrated in figure above. As said earlier, two Bell states are exactly identified by this scheme and the remaining two only together, as demonstrated in [10]. The antisymmetric state  $|\psi^-\rangle$  is easily identified, as only in this case the two photons are detected in separate output ports of the beam splitter. However in the case of  $|\psi^+\rangle$  the photons will emerge from the same output port of the beam splitter, but they will still have the orthogonal polarizations in the H,V-Basis. For this case additional polarization beam splitters (PBS) are introduced at the output ports of the BS and two interfering photons will

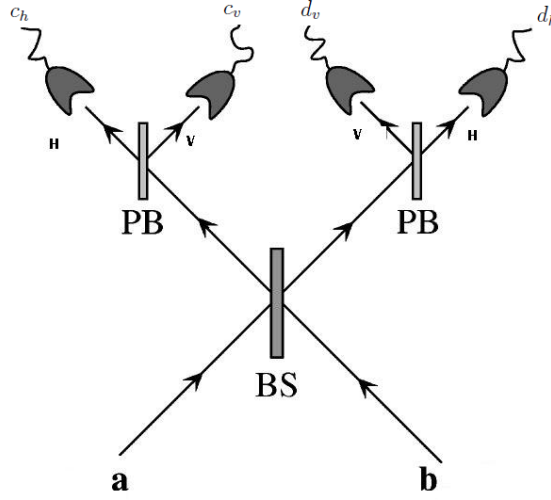


Figure 2.8: Bell state measurement.

be found in the separate outputs of the polarizer respectively and emerge from the BS via  $c$  and  $d$  modes. Only when two input photons are entangled in the antisymmetric state, will take the separate output modes and consequently lead to a coincidence detection in two detectors. More specifically, when a photon is detected in either of the output ports of BS, and in the opposite outputs of PBS then  $|\psi^-\rangle$  state is observed (either the detectors  $c_h$  and  $d_v$  fire, or  $c_v$  and  $d_h$ ). On the other hand, if two photons are detected in the same output port of BS and different output of the PBS then  $|\psi^+\rangle$  will be observed (either  $c_h$  and  $c_v$  fire, or  $d_h$  and  $d_v$ ). Here for state  $|\psi^-\rangle$  by following the sequence of detections HVVH for  $a$  and  $d$  modes is

$$|\psi^-\rangle = \frac{1}{\sqrt{2}} [ |0101\rangle - |1010\rangle ], \quad (2.7.1)$$

$$|\psi^-\rangle = \frac{1}{\sqrt{2}} [ \hat{a}_v^\dagger \hat{b}_h^\dagger |0000\rangle - \hat{a}_h^\dagger \hat{b}_v^\dagger |0000\rangle ]. \quad (2.7.2)$$

Now applying the beam splitter transformation which has been described in the previous section, the above equation will become

$$\begin{aligned} |\psi^-\rangle &\xrightarrow{B^\dagger} \frac{1}{\sqrt{2}} \left[ \frac{(\hat{a}_v^\dagger + i\hat{b}_v^\dagger)(i\hat{a}_h^\dagger + \hat{b}_h^\dagger)}{2} |0000\rangle - \frac{(\hat{a}_h^\dagger + i\hat{b}_h^\dagger)(i\hat{a}_v^\dagger + \hat{b}_v^\dagger)}{2} |0000\rangle \right], \\ &= \frac{1}{2\sqrt{2}} \left[ (i\hat{a}_v^\dagger \hat{a}_h^\dagger + \hat{a}_v^\dagger \hat{b}_h^\dagger - \hat{b}_v^\dagger \hat{a}_h^\dagger + i\hat{b}_v^\dagger \hat{b}_h^\dagger) |0000\rangle - (i\hat{a}_h^\dagger \hat{a}_v^\dagger + \hat{a}_h^\dagger \hat{b}_v^\dagger - \hat{b}_h^\dagger \hat{a}_v^\dagger + i\hat{b}_h^\dagger \hat{b}_v^\dagger) |0000\rangle \right], \end{aligned}$$



$$\begin{aligned}
|\psi^-\rangle &= \frac{1}{2\sqrt{2}} [i|1100\rangle + |0101\rangle - |1010\rangle + i|0011\rangle - i|1100\rangle - |1010\rangle + |0101\rangle - i|0011\rangle], \\
&= \frac{1}{\sqrt{2}} [|0101\rangle - |1010\rangle].
\end{aligned} \tag{2.7.3}$$

Hence this equation shows that the photons will emerge from different output ports of the beam splitter.

Now to detect state  $|\psi^+\rangle$ ,

$$|\psi^+\rangle = \frac{1}{\sqrt{2}} [|0101\rangle + |1010\rangle], \tag{2.7.4}$$

$$|\psi^+\rangle = \frac{1}{\sqrt{2}} [\hat{a}_v^\dagger \hat{b}_h^\dagger |0000\rangle + \hat{a}_h^\dagger \hat{b}_v^\dagger |0000\rangle]. \tag{2.7.5}$$

In a similar way as we did for  $|\psi^-\rangle$  using the beam splitter transformation

$$\begin{aligned}
|\psi^+\rangle &\xrightarrow{B^\dagger} \frac{1}{\sqrt{2}} \left[ \frac{(\hat{a}_v^\dagger + i\hat{b}_v^\dagger)(i\hat{a}_h^\dagger + \hat{b}_h^\dagger)}{2} |0000\rangle - \frac{(\hat{a}_h^\dagger + i\hat{b}_h^\dagger)(i\hat{a}_v^\dagger + \hat{b}_v^\dagger)}{2} |0000\rangle \right], \\
&= \frac{1}{2\sqrt{2}} \left[ (i\hat{a}_v^\dagger \hat{a}_h^\dagger + \hat{a}_v^\dagger \hat{b}_h^\dagger - \hat{b}_v^\dagger \hat{a}_h^\dagger + i\hat{b}_v^\dagger \hat{b}_h^\dagger) |0000\rangle - (i\hat{a}_h^\dagger \hat{a}_v^\dagger + \hat{a}_h^\dagger \hat{b}_v^\dagger - \hat{b}_h^\dagger \hat{a}_v^\dagger + i\hat{b}_h^\dagger \hat{b}_v^\dagger) |0000\rangle \right], \\
&= \frac{1}{2\sqrt{2}} [i|1100\rangle + |0101\rangle - |1010\rangle + i|0011\rangle + i|1100\rangle + |1010\rangle - |0101\rangle + i|0011\rangle], \\
|\psi^+\rangle &= \frac{1}{\sqrt{2}} [|1100\rangle + |0011\rangle].
\end{aligned} \tag{2.7.6}$$

This resulting state is quite different from the state  $|\psi^-\rangle$  because the photons emerge from the same output port of the beam splitter. For the states  $|\phi^\pm\rangle$  the photons will strike the detector after emerging from the same output port of the beam splitter.

Thus the state detected at the detectors after passing through BS can be found as

$$|\phi^\pm\rangle = \frac{1}{\sqrt{2}} [|1001\rangle \pm |0110\rangle], \tag{2.7.7}$$

$$|\phi^\pm\rangle = \frac{1}{\sqrt{2}} [\hat{a}_h^\dagger \hat{b}_h^\dagger |0000\rangle \pm \hat{a}_v^\dagger \hat{b}_v^\dagger |0000\rangle], \tag{2.7.8}$$

$$|\phi^\pm\rangle = \frac{1}{2\sqrt{2}} [(i\hat{a}_h^\dagger + i\hat{b}_h^\dagger)(i\hat{a}_h^\dagger + \hat{b}_h^\dagger) |0000\rangle \pm (\hat{a}_v^\dagger + i\hat{b}_v^\dagger)(i\hat{a}_v^\dagger + \hat{b}_v^\dagger) |0000\rangle]. \tag{2.7.9}$$

For state  $|\phi^+\rangle$

$$\begin{aligned}
|\phi^+\rangle &= \frac{1}{2\sqrt{2}} [(i\hat{a}_h^\dagger \hat{a}_h^\dagger + \hat{a}_h^\dagger \hat{b}_h^\dagger - \hat{b}_h^\dagger \hat{a}_h^\dagger + i\hat{b}_h^\dagger \hat{b}_h^\dagger) |0000\rangle \\
&\quad + (i\hat{a}_v^\dagger \hat{a}_v^\dagger + \hat{a}_v^\dagger \hat{b}_v^\dagger - \hat{b}_v^\dagger \hat{a}_v^\dagger + i\hat{b}_v^\dagger \hat{b}_v^\dagger) |0000\rangle],
\end{aligned} \tag{2.7.10}$$

$$|\phi^+\rangle = \frac{1}{2\sqrt{2}}[i\sqrt{2}|2000\rangle + |1001\rangle - |1001\rangle + i\sqrt{2}|0002\rangle + i\sqrt{2}|0200\rangle + |0110\rangle - |0110\rangle + i\sqrt{2}|0020\rangle], \quad (2.7.11)$$

$$|\phi^+\rangle = \frac{i}{2}[|2000\rangle + |0002\rangle + |0200\rangle + |0020\rangle]. \quad (2.7.12)$$

For state  $|\phi^-\rangle$ ,

$$|\phi^-\rangle = \frac{1}{2\sqrt{2}}[i\sqrt{2}|2000\rangle + |1001\rangle - |1001\rangle + i\sqrt{2}|0002\rangle - i\sqrt{2}|0200\rangle - |0110\rangle + |0110\rangle - i\sqrt{2}|0020\rangle], \quad (2.7.13)$$

$$|\phi^-\rangle = \frac{i}{2}[|2000\rangle + |0002\rangle - |0200\rangle - |0020\rangle]. \quad (2.7.14)$$

Since, as described earlier, state  $|\psi^-\rangle$  has an antisymmetric spatial part, so only this state will register coincidence clicks, while the other three Bell states follow the bosonic statistics so they cannot be distinguished from each other. The photons for the state  $|\phi^+\rangle$  or in  $|\phi^-\rangle$  will also leave the BS in the same output port, will have the same polarization in H,V-Basis. Thus we can discriminate the states  $|\psi^-\rangle$  and  $|\phi^\pm\rangle$  only by a polarization analysis in H,V-Basis using PBS. The detection scheme of these four Bell states is given in the table below,

Detector's click			Could have been triggered by
$c_h$	and	$d_h$	$ \psi^-\rangle$
$c_v$	and	$d_v$	$ \psi^-\rangle$
$c_h$	and	$c_v$	$ \psi^+\rangle$
$d_v$	and	$d_h$	$ \psi^+\rangle$
$c_h$	sees	2 photons	$ \phi^-\rangle$ $ \phi^+\rangle$
$c_v$	sees	2 photons	$ \phi^-\rangle$ $ \phi^+\rangle$
$d_h$	sees	2 photons	$ \phi^-\rangle$ $ \phi^+\rangle$
$d_v$	sees	2 photons	$ \phi^-\rangle$ $ \phi^+\rangle$

Table 2.1: Table showing the clicks at various detectors for various incident Bell states.

## 2.8 Detector Model

Now we discuss the theory of imperfect detectors which are being used to detect photons in different quantum information processing experiments. The theory of imperfect detectors used for swapping and dense coding experiments will be discussed in detail. The InGaAs (Indium-Gallium-Arsenide) avalanche photodiodes detectors (APD,s) [25] are semiconductor based photon detectors that are being used in different experiments and can efficiently detect single photons at close to room temperature. These detectors use strong electric fields to accelerate the electrons flowing in the semiconductor. When a single-photon strikes the detector, an avalanche of electrons is generated that readily triggers a *click or no-click*, indicating the arrival of the photon. Ideal detectors are still a technological challenge. Detectors also exhibit dark counts i.e click with no photon striking the detector. The dark count probability of the detector is measured before incorporating it into the experiment and the effect of these events is taken into account. Here we model such an imperfect detector by placing a beam splitter in front of a perfect detector. This beam splitter causes the interference of the coherent input signal state with a thermal state, representing the dark counts and the random errors that occur. The detection probabilities produced by these theoretical imperfect detector agree with those derived from an experimental detectors while providing a useful generalization. Now we are going to discuss the detectors in some detail.

### 2.8.1 Ideal Photon-number Discriminating Detectors

Ideal photon number discriminating detectors [26] are such that they never click when there is a vacuum and always click when there are photons present in a certain mode. The strength of the click provides information about the number of photons present in that mode. They are mathematically represented by photon counting projection valued measurement (PVMs)

$$\hat{\Pi}_n = |n\rangle\langle n|, \quad n = 0, 1, 2, 3, \dots \quad (2.8.1)$$

with respect to the Fock state basis  $\{|n\rangle, n \in N_0\}$  of a certain mode.

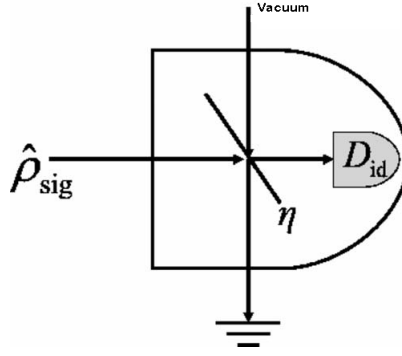


Figure 2.9: A model for an imperfect detector with efficiency  $\eta$  and dark counts generated by a fictitious thermal background source. The signal mode and the thermal mode represented by the quantum states  $\rho_{sig}$  and  $\rho_T$ , respectively, meet at a beam splitter with transmittance  $\eta$ . One of its exits is directed to a perfect (ideal) detector ( $D_{id}$ ); the photons of the second exit port are discarded. The perfect detector is assumed to be a unit-efficiency photon detector with no dark counts. We will make a distinction of two cases. In the first instance we will assume the perfect detector to be photon-number discriminating. Later we consider the case where the perfect detector is a unit-efficiency threshold detector.

## 2.8.2 Inefficient Photon-number Discriminating Detectors with no Dark Counts

Inefficient photon number discriminating detectors have nonunit efficiency  $\eta$  ( $0 < \eta < 1$ ), meaning that even if photons are incident into the detector it has a finite probability not to trigger a click. The model of such imperfect detectors is given in [26] by placing a beam splitter (BS) with transmittance  $\eta$  before an ideal detector (with efficiency  $\eta = 1$ ). Here  $\eta$  is used both for transmittance of beam splitter and efficiency of detector. The model of such a detector is shown in Fig.(2.9).

Now the probability of such a detector can be calculated as

$$P_{\eta}(q|\rho_{sig}) = Tr_{trans}\left\{\prod_q Tr_{ref}[\hat{U}_{BS}(\eta)(\rho_{sig} \otimes |vac\rangle\langle vac|)U_{BS}^{\dagger}(\eta)]\prod_q\right\}, \quad (2.8.2)$$

where,  $U_{BS}(\eta)$  is the unitary evolution of the BS

$$\hat{U}_{BS}(\eta) = \begin{pmatrix} \cos \frac{\theta}{2} & i \sin \frac{\theta}{2} \\ -i \sin \frac{\theta}{2} & \cos \frac{\theta}{2} \end{pmatrix}, \quad (2.8.3)$$

and  $\rho_{sig}$  is the input signal mode and it is photon number Fock state  $\rho_{sig} = |i\rangle\langle i|$ . The conditional probability to detect  $q$  photons is  $P_{\eta}(q|i) = \delta_{qi}$  with unit efficiency detectors and with  $\eta$ -efficiency detectors ( $\eta \neq 1$ )

$$P_{\eta}(q|i) = Tr_{trans}\left\{\prod_q Tr_{ref}[\hat{U}_{BS}(\eta)(|i\rangle\langle i| \otimes |vac\rangle\langle vac|)U_{BS}^{\dagger}(\eta)]\prod_q\right\}, \quad (2.8.4)$$

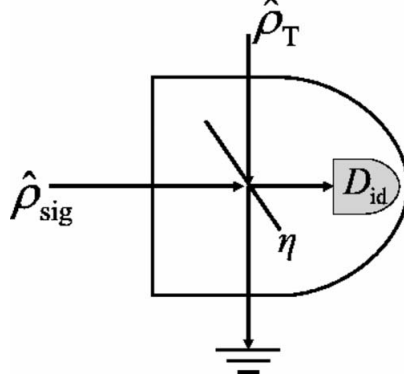


Figure 2.10: Model of imperfect detector with thermal background.

$$P_{\eta}(q|i) = \begin{cases} \binom{i}{q} \eta^q (1-\eta)^{i-q} & \text{if } i \geq q \\ 0 & \text{if } i < q \end{cases} \quad (2.8.5)$$

It is clear from Eq.(2.8.5) that in order to detect  $q$  photons the number of incident photons  $i$  must be greater than  $q$  as the dark counts are not included yet.

It should be noted that all the possible inefficiencies of the experiment are taken into account the detector's efficiency,  $\eta$ . Thus efficiency of this model is to be understood as the effective efficiency comprising the proper intrinsic detector efficiencies as well as all kinds of other losses.

### 2.8.3 Inefficient Photon-number Discriminating Detectors with Dark Counts

In order to take into account the possibility of dark counts, we combine the signal mode, which is to be measured, with a thermal state of the form given below, instead of using vacuum states.

$$\hat{\rho}_T = \frac{1}{\cosh^2 r} \sum_{n=0}^{\infty} \tanh^{2n} r |n\rangle \langle n|. \quad (2.8.6)$$

The detector model is shown in the Fig.(2.10). Dark counts are the result of photons incident onto the detector from the environment i.e the thermal background, is responsible for the dark counts, is entirely fictitious and does not have to correspond to a real actually existing photonic field.

Using this detector model we can find the conditional probability of photon-number discriminating detector having efficiency  $\eta$  and dark count probability  $\rho_{dc}$ , according to

$$P_{\eta,r}(q|i) = Tr_{trans}\left\{\prod_q Tr_{ref}[\hat{U}_{BS}(\eta)(|i\rangle\langle i| \otimes \rho_T)\hat{U}_{BS}^\dagger(\eta)]\prod_q\right\}. \quad (2.8.7)$$

The dark count probability of a non ideal threshold detectors amounts to

$$\rho_{dc} = \frac{(1-\eta)\tanh^2 r}{1-\eta\tanh^2 r} = \frac{(1-\eta)\exp[-\frac{\hbar\omega}{KT}]}{1-\eta\exp[-\frac{\hbar\omega}{KT}]}. \quad (2.8.8)$$

For the purpose of modeling realistic entanglement swapping it is sufficient to know the conditional probability of a particular state i.e Fock state  $\rho_{sig} = |i\rangle\langle i|$ . Thus, the conditional probability to detect  $q$  photons given that  $i$  photons are incident on the detector with efficiency  $\eta$  is written as  $P_{\eta,\rho_{dc}}(q|i)$ . One important fact which needs to be mentioned here is that in this case  $q$  may be greater than  $i$  due to the dark counts.

$$P_{\eta,r}(q|\rho_{sig}) = Tr_{trans}\left\{\prod_q Tr_{ref}[\hat{U}_{BS}(\eta)(\rho_{sig} \otimes \rho_T)\hat{U}_{BS}^\dagger(\eta)]\prod_q\right\}. \quad (2.8.9)$$

Here  $P_{\eta,r}(q|i)$  notation is being used to represent conditional probability. However later it will clear how  $\rho_{dc}$  emerges in the final expression using Eq.(2.8.8).

Let  $\hat{c}, \hat{c}^\dagger$  and  $\hat{e}, \hat{e}^\dagger$  are the annihilation and creation operators of the signal and thermal fictitious background modes respectively and the input signal state will be represented as  $\rho_{sig,T}^{in}$ . The unitary evolution of beam splitter  $\hat{U}_{BS}(\eta)$  acts on these creation and annihilation operators as

$$\begin{pmatrix} \hat{c} \\ \hat{e} \end{pmatrix} \rightarrow B_\eta^\dagger \begin{pmatrix} \hat{c} \\ \hat{e} \end{pmatrix} \begin{pmatrix} \hat{c}^\dagger \\ \hat{e}^\dagger \end{pmatrix} \rightarrow B_\eta^T \begin{pmatrix} \hat{c}^\dagger \\ \hat{e}^\dagger \end{pmatrix},$$

where beam splitter transformation matrix consisting of transmission  $T = \sqrt{\eta}$  and reflection  $R = \sqrt{1-\eta}$  coefficients is

$$B_\eta = \begin{pmatrix} \sqrt{\eta} & \sqrt{1-\eta} \\ -\sqrt{1-\eta} & \sqrt{\eta} \end{pmatrix},$$

$$\begin{aligned}
\rho_{sig,T}^{out} &:= \hat{U}_{BS}(\eta)\rho_{sig,T}^{in}\hat{U}_{BS}^\dagger(\eta), \\
&= \frac{1}{\cosh^2 r} \sum_{n=0}^{\infty} \frac{\tanh^{2n} r}{i!n!} (\sqrt{\eta}\hat{c}^\dagger - \sqrt{1-\eta}\hat{e}^\dagger)^i \\
&\quad (\sqrt{1-\eta}\hat{c}^\dagger + \sqrt{\eta}\hat{e}^\dagger)^n |vac\rangle\langle vac| \\
&\quad (\sqrt{1-\eta}\hat{c} + \sqrt{\eta}\hat{e})^n (\sqrt{\eta}\hat{c} - \sqrt{1-\eta}\hat{e})^i, \\
\rho_{sig,T}^{out} &= \frac{1}{\cosh^2 r} \sum_{n=0}^{\infty} \frac{\tanh^{2n} r}{i!n!} \sum_{\nu=0}^i \sum_{\nu'=0}^i \sum_{\mu=0}^n \sum_{\mu'=0}^n \binom{i}{\nu} \binom{i}{\nu'} \binom{n}{\mu} \binom{n}{\mu'} (-1)^{\nu+\nu'} \\
&\quad (\sqrt{\eta})^{2n+\nu+\nu'-\mu-\mu'} (\sqrt{1-\eta})^{2i-\nu-\nu'+\mu+\mu'} \\
&\quad \times (\hat{c}^\dagger)^{\nu+\mu} (\hat{e}^\dagger)^{i+n-\nu-\mu} |vac\rangle\langle vac| (\hat{e}^\dagger)^{i+n-\nu'-\mu'} (\hat{c}^\dagger)^{\nu'+\mu'}, \\
\rho_{sig,T}^{out} &= \frac{1}{\cosh^2 r} \sum_{n=0}^{\infty} \frac{\tanh^{2n} r}{i!n!} \sum_{\nu=0}^i \sum_{\nu'=0}^i \sum_{\mu=0}^n \sum_{\mu'=0}^n \binom{i}{\nu} \binom{i}{\nu'} \binom{n}{\mu} \binom{n}{\mu'} (-1)^{\nu+\nu'} \\
&\quad \times (\sqrt{\eta})^{2n+\nu+\nu'-\mu-\mu'} (\sqrt{1-\eta})^{2i-\nu-\nu'+\mu+\mu'} \sqrt{(\nu+\mu)!} \\
&\quad \times \sqrt{(\nu'+\mu')!} \sqrt{(i+n-\nu-\mu)!} \sqrt{(i+n-\nu'-\mu')!} \\
&\quad \times |\nu+\mu, i+n-\nu-\mu\rangle\langle \nu'+\mu', i+n-\nu'-\mu'|.
\end{aligned}$$

Now according to Eq.(2.8.9), ignoring the reflected mode and taking the projection on Fock state  $|q\rangle$  and finally taking the trace over transmission mode we get this result

$$P_{\eta,r}(q|i) = \frac{1}{\cosh^2 r} \left(\frac{\eta}{1-\eta}\right)^q (i-\eta)^i \sum_{n=0}^{\infty} [\eta \tanh^2 r]^n \frac{q!(i+n-q)!}{i!n!} [\Omega(\eta, i, q, n)]^2 \quad (2.8.10)$$

where

$$\Omega(\eta, i, q, n) := \sum_{\mu=0}^n \binom{i}{q-\mu} \binom{n}{\mu} \left(\frac{\eta-1}{\eta}\right)^\mu. \quad (2.8.11)$$

It is important to note that  $\Omega(\eta, i, q, n) = 0$  unless  $i \geq q - n$ . This is quite straight forward result: the number of detected photons in  $D_{id}$  cannot be greater than the sum  $(i+n)$  of signal and thermal photons. Before we proceed, let us distinguish the two cases:  $i \geq q$  and  $i < q$ .

For  $i \geq q$ , let

$$\Omega(\eta, i, q, n) = \sum_{\mu=0}^n \binom{i}{q-\mu} \binom{n}{n+1} \left(\frac{\eta-1}{\eta}\right)^\mu. \quad (2.8.12)$$

The above expression of  $\Omega(\eta, i, q, n)$  can be written as,

$$\Omega(\eta, i, q, n) = \sum_{\mu=0}^n \frac{i!}{(q-\mu)!(i-q-\mu)!} \frac{n!}{\mu!(n-\mu)!} \left(\frac{\eta-1}{\eta}\right)^\mu \quad (2.8.13)$$

Now we try to write this result in terms of Hypergeometric function  $F_1(., .; .; .)$  just to make it more compact where Hypergeometric function is defined as,

$$F_1(\alpha, \beta; \gamma; z) := 1 + \sum_{n=1}^{\infty} \frac{(\alpha)_n (\beta)_n z^n}{(\gamma)_n n!},$$

where  $(\alpha)_n := \Gamma(\alpha+n)/\Gamma(\alpha)$  is the Pochhammer symbol;  $\Gamma$  is the gamma function. The variable  $\mu$  should go up to infinity to write the above expression into Hypergeometric function terms but for  $\mu > n$  all the terms will vanish as  $\mu$  can go max. to  $n$ . To get finite value of the series given in Eq.(2.8.13) we make  $q$  and  $n$  both negative using the properties of gamma function,

$$\frac{q!}{(q-\mu)!} = \frac{\Gamma(q+1)}{\Gamma(q-\mu+1)} = \frac{\Gamma(-q+\mu)}{\Gamma(-q)} (-1)^\mu.$$

Similarly

$$\frac{n!}{(n-\mu)!} = \frac{\Gamma(n+1)}{\Gamma(n-\mu+1)} = \frac{\Gamma(-n+\mu)}{\Gamma(-n)} (-1)^\mu.$$

Now multiplying and dividing Eq.(2.8.13) by  $q!(q-i)!$ , we have

$$\Omega(\eta, i, q, n) = \sum_{\mu=0}^n \frac{i!q!}{(q-i)!(q-\mu)!(i-q-\mu)!} \frac{n}{(n-\mu)!(q-i)!} \left(\frac{\eta-1}{\eta}\right)^\mu.$$

Hence

$$\Omega(\eta, i, q, n) = \binom{i}{q} {}_2F_1\left(-n, -q; i-q+1; \frac{\eta-1}{\eta}\right). \quad (2.8.14)$$

Now for  $q > i$ , we have

$$\begin{aligned} \Omega(\eta, i, q, n) &:= \sum_{\mu=q-i}^n \binom{i}{q-\mu} \binom{n}{\mu} \left(\frac{\eta-1}{\eta}\right)^\mu, \\ &= \sum_{\mu=q-i}^n \frac{i!}{(q-\mu)!(1-q+\mu)!} \frac{n!}{\mu!(n-\mu)!} \left(\frac{\eta-1}{\eta}\right)^\mu. \end{aligned} \quad (2.8.15)$$



By introducing  $k = \mu - q + i$ , we have

$$\Omega(\eta, i, q, n) = \sum_{k=0}^{n-q+i} \frac{i!}{k!(i-k)!} \frac{n!}{(k+q-i)!(n-q-k+i)!} \left(\frac{\eta-1}{\eta}\right)^{k+q-i}. \quad (2.8.16)$$

Mutiplied and dividing above equation by  $(q-i)!(n-q-i)!$

$$\begin{aligned} \Omega(\eta, i, q, n) &= \sum_{k=0}^{n-q+i} \frac{i!(q-i)!}{k!(i-k)!(n-q-i)!} \frac{n!(n-q-i)!}{(k+q-i)!(n-q-k+i)!(q-i)!} \left(\frac{\eta-1}{\eta}\right)^{k+q-i}, \\ &= \sum_{k=0}^{n-q+i} \left(\frac{\eta-1}{\eta}\right)^{q-i} \binom{n}{q-i} {}_2F_1(-i, n-q+i; q-i+1; \frac{\eta-1}{\eta}). \end{aligned} \quad (2.8.17)$$

Here  $k$  is a dummy index so changing  $k \rightarrow \mu$ , our final result will become

$$\begin{aligned} \Omega(\eta, i, q, n) &= \sum_{\mu=0}^{n-q+i} \left(\frac{\eta-1}{\eta}\right)^{q-i} \binom{n}{q-i} \\ &\quad \times {}_2F_1(-i, n-q+i; q-i+1; \frac{\eta-1}{\eta}). \end{aligned} \quad (2.8.18)$$

Now inserting Eq.(2.8.14) into Eq.(2.8.10) and utilizing the notation  $\tilde{b}(\eta, r) := \eta \tanh^2 r$ , we get this result for  $i \geq q$ , Now in the similar way, for  $q > i$

$$\begin{aligned} P_{\eta, r}(q|i) &= \frac{1}{\cosh^2 r} \left(\frac{\eta-1}{\eta}\right)^{q-i} \eta^i \sum_{n=q-i}^{\infty} \binom{q}{i} \binom{n}{q-i} \\ &\quad [\tilde{b}(\eta, r)]^n [{}_2F_1(-i, n-q+i; q-i+1; \frac{\eta-1}{\eta})]^2, \end{aligned} \quad (2.8.19)$$

$$\begin{aligned} P_{\eta, r}(q|i) &= \frac{1}{\cosh^2 r} \left(\frac{\eta-1}{\eta}\right)^{q-i} \eta^i [\tilde{b}(\eta, r)]^{q-i} \sum_{m=0}^{\infty} \binom{q}{i} \binom{q-i+m}{q-i} \\ &\quad [\tilde{b}(\eta, r)]^m [{}_2F_1(-i, -m; q-i+1; \frac{\eta-1}{\eta})]^2, \end{aligned} \quad (2.8.20)$$

$$\begin{aligned} P_{\eta, r}(q|i) &= \frac{1}{\cosh^2 r} \left(\frac{\eta-1}{\eta}\right) b^{\sim}(\eta, r)^{q-i} \eta^i \sum_{n=0}^{\infty} \binom{q}{i} \binom{q-i+n}{q-i} \\ &\quad [\tilde{b}(\eta, r)]^n [{}_2F_1(-n, -i; q-i+1; \frac{\eta-1}{\eta})]^2. \end{aligned} \quad (2.8.21)$$

In the last step, after renaming the indices from  $m \rightarrow n$ , we used the permutation symmetry property of hypergeometric functions

$${}_2F_1(\alpha, \beta; \gamma; z) = {}_2F_1(\beta, \alpha; \gamma; z),$$

to bring that expression into the desired form of probability. This permutation property shows that there exists a partial symmetry between two results for two different cases discussed above.

Replacing the dependence of probability on parameter  $r$  of the thermal source by probability of dark count  $\rho_{dc}$ , using

$$b(\eta, \rho_{dc}) := \tilde{b}[\eta, r(\eta, \rho_{dc})] = \eta \tanh^2 r = \left[1 + \frac{1 - \eta}{\eta \rho_{dc}}\right]^{-1},$$

and Eq.(2.8.8), we get

$$\frac{1}{\cosh^2 r} = \frac{(1 - \eta)(1 - \rho_{dc})}{1 - \eta(1 - \rho_{dc})}.$$

Finally by introducing these definitions into Eq.(2.8.10) and Eq.(2.8.22), we get the desired form of the conditional probabilities depending on dark counts for photon number discriminating detectors.

$$P_{\eta, \rho_{dc}}(q|i) = \begin{cases} \frac{(1-\eta)(1-\rho_{dc})}{1-\eta(1-\rho_{dc})} \left(\frac{\eta}{1-\eta}\right)^q (1-\eta)^i \Omega(i, q; \eta, \rho_{dc}) & \text{if } i \geq q \\ \frac{(1-\eta)(1-\rho_{dc})}{1-\eta(1-\rho_{dc})} \left[\frac{1-\eta}{\eta} b(\eta, \rho_{dc})\right]^{q-i} \eta^i \Omega(q, i; \eta, \rho_{dc}) & \text{if } q \geq i \end{cases}, \quad (2.8.22)$$

where

$$\Omega(i, q; \eta, \rho_{dc}) = \sum_{n=0}^{\infty} \binom{i}{q} \binom{i - q + n}{i - q} [b^{\sim}(\eta, r)]^n [{}_2F_1(-n, -q; i - q + 1; \frac{\eta - 1}{\eta})]^2, \quad (2.8.23)$$

$$\Omega(q, i; \eta, \rho_{dc}) = \sum_{n=0}^{\infty} \binom{q}{i} \binom{q - i + n}{q - i} [\tilde{b}(\eta, r)]^n [{}_2F_1(-n, -i; q - i + 1; \frac{\eta - 1}{\eta})]^2. \quad (2.8.24)$$

#### 2.8.4 Inefficient Threshold Detectors with Dark Counts

Threshold detectors are more easily available than the photon number discriminating detectors which are a technological challenge and their realization is still in its

infancy. To provide a practically relevant entanglement swapping process we have to consider threshold detectors [26]. In the ideal scenario these detectors effectively measure whether there is no photon or at least one photon in a mode. Unit efficiency threshold detectors with no dark counts are referred as ideal threshold detectors (ITD), and mathematically these are represented as,

$$\hat{\Pi}_0 = |0\rangle\langle 0|, \quad \hat{\Pi}_0^\perp = 1 - \hat{\Pi}_0. \quad (2.8.25)$$

Inefficient threshold detectors can be realized using the same detector model as above, but now replacing  $D_{id}$  with ITD. The relevant conditional probabilities can be calculated in the same manner as we did in the case of photon number discriminating detectors, but now with  $q$  being either the event “no click” or “click” corresponding to the PVM elements  $\hat{\Pi}_0$  or  $\hat{\Pi}_0^\perp$  respectively. Again for the purpose of entanglement swapping, we calculate the conditional probabilities for the input signal  $\hat{\rho}_{sig} = |i\rangle\langle i|$ . The conditional probabilities of recording “no click” can be calculated directly from Eq.(2.8.22) by setting  $q = 0$ . And the probability for the event “click” will just be one minus the latter probability

$$\begin{aligned} P_{\eta, \rho_{dc}}(no - click|i) &= P_{\eta, \rho_{dc}}(q = 0|i) \\ &= (1 - \rho_{dc})[1 - \eta(1 - \rho_{dc})]^i, \end{aligned} \quad (2.8.26)$$

$$\begin{aligned} P_{\eta, \rho_{dc}}(click|i) &= 1 - P_{\eta, \rho_{dc}}(no - click|i) \\ &= (1 - \rho_{dc})[1 - \eta(1 - \rho_{dc})]^i. \end{aligned} \quad (2.8.27)$$

We will calculate the conditional probabilities under realistic conditions for swapping process and then by just plugging those values here in above expressions we will get required probabilities of photon detection under most practical conditions.

# Chapter 3

## Realistic Entanglement Swapping

### 3.1 Introduction

Entanglement has been realized either by having the two entangled particles emerge from a single source [1,27], or by having two particles interact with each other [28,29]. But entanglement can also be obtained by making use of the projection of the state of the two particles onto an entangled state. The main advantage of this projection measurement is that it does not necessarily require a direct interaction between the two particles. When each of the two particles is entangled with another partner particle an appropriate measurement, for example a Bell measurement, of the partner particles will automatically collapse the state of the remaining two particles into an entangled state. This amazing application of the projection postulate is referred to as entanglement swapping [3,30].

The theoretical description of entanglement swapping generally requires the components, used in experimental set up, ideal. But in the case of realistic entanglement swapping, the sources, detectors and other components used in the experimental setup are considered non ideal. In this chapter we will see how the realistic entanglement swapping procedure can be modeled by taking into account all the inefficiencies. We will also discuss Bell measurement process here.

## 3.2 Theoretical Entanglement Swapping

Entanglement swapping is an interesting extension of teleportation. It can make two particles entangled together that have neither interacted in past. This is possible even if the particles are light years apart.

Consider two EPR pairs which are labeled as 1,2 and 3,4 where 1,2 are entangled and 3,4 are entangled together. Let's also consider that Alice has qubits 1 and 4 in her possession and Bob has other two qubits in his possession. Qubits 1 and 2 are in the following Bell state

$$|\beta_{00}\rangle_{12} = \frac{|00\rangle_{12} + |11\rangle_{12}}{\sqrt{2}}. \quad (3.2.1)$$

Similarly the qubits 3 and 4 are in the state

$$|\beta_{00}\rangle_{34} = \frac{|00\rangle_{34} + |11\rangle_{34}}{\sqrt{2}}. \quad (3.2.2)$$

These two states are maximally entangled Bell states. The product of these two states would be

$$\begin{aligned} |\beta_{00}\rangle_{12}|\beta_{00}\rangle_{34} &= \left( \frac{|00\rangle_{12} + |11\rangle_{12}}{\sqrt{2}} \right) \left( \frac{|00\rangle_{34} + |11\rangle_{34}}{\sqrt{2}} \right), \\ (|\beta_{00}\rangle_{12})(|\beta_{00}\rangle_{34}) &= \frac{|00\rangle_{12}|00\rangle_{34} + |00\rangle_{12}|11\rangle_{34} + |11\rangle_{12}|00\rangle_{34} + |11\rangle_{12}|11\rangle_{34}}{2}. \end{aligned} \quad (3.2.3)$$

Now by doing some simple algebra and rearranging qubits by writing qubits 1 and 4 together and 2 and 3 together, we have

$$(|\beta_{00}\rangle_{12})(|\beta_{00}\rangle_{34}) = \frac{1}{2}(|00\rangle_{14}|00\rangle_{23} + |01\rangle_{14}|01\rangle_{23} + |10\rangle_{14}|10\rangle_{23} + |11\rangle_{12}|11\rangle_{34}). \quad (3.2.4)$$

Notice that, the product of  $|\beta_{00}\rangle_{14}$  with  $|\beta_{00}\rangle_{23}$  is

$$\begin{aligned} (|\beta_{00}\rangle_{14})(|\beta_{00}\rangle_{23}) &= \left( \frac{|00\rangle_{14} + |11\rangle_{14}}{\sqrt{2}} \right) \left( \frac{|00\rangle_{23} + |11\rangle_{23}}{\sqrt{2}} \right), \\ &= \frac{|00\rangle_{14}|00\rangle_{23} + |00\rangle_{14}|11\rangle_{23} + |11\rangle_{14}|00\rangle_{23} + |11\rangle_{14}|11\rangle_{23}}{2}. \end{aligned}$$

The above equation shows that  $|\beta_{00}\rangle_{12}|\beta_{00}\rangle_{34}$  is missing few terms in their product but we can stick them in there by adding and subtracting these terms. Then again after doing some simple calculations, the result will be

$$(|\beta_{00}\rangle_{12})(|\beta_{00}\rangle_{34}) = \frac{1}{2} \times (|\beta_{00}\rangle_{14}|\beta_{00}\rangle_{23} + |\beta_{10}\rangle_{14}|\beta_{10}\rangle_{23} + |\beta_{01}\rangle_{14}|\beta_{01}\rangle_{23} + |\beta_{11}\rangle_{14}|\beta_{11}\rangle_{23}).$$

Remember that Alice has particles 1 and 4 in her possession and Bob has particles 2 and 3 in his possession. Then Alice does a Bell measurement on the qubits in her possession. Depending on the results of Alice's measurement  $|\beta_{00}\rangle_{14}$ ,  $|\beta_{01}\rangle_{14}$ ,  $|\beta_{10}\rangle_{14}$ ,  $|\beta_{11}\rangle_{14}$ , Bob's system collapses into one of the four Bell states which shows that particle 2 and 3 are entangled as is clear from the above equation.

### 3.3 Realistic Entanglement Swapping

This theory is based on the work by Artur Scherer et al. [3] explaining realistic entanglement swapping. The physical situation for a practical entanglement swapping process is shown in Fig.(3.1). As we are going to discuss the entanglement swapping process in realistic scenario therefore the parametric down-conversion sources and detectors shown in the Fig.(3.1) are considered realistic. The PDC sources and detectors have been discussed in detail in chapter 2 in this scenario. The two PDC sources generate photons into spatial modes  $a$ ,  $b$ ,  $c$  and  $d$ , where  $a$  and  $b$  corresponds to first source and  $c$  and  $d$  to the second source. Also the photons  $(a, b)$  and  $(c, d)$  are entangled with each other. To perform entanglement swapping, a joint Bell state measurement is performed on  $b$  and  $c$  modes at the beam splitter and the resulting state projects  $a$  and  $d$  modes on to an entangled state. As a result the photons in the  $a$  and  $d$  modes become entangled despite having no common past [3]. The entanglement initially present in  $(a, b)$  and  $(c, d)$  modes is now swapped on  $a$  and  $d$  modes. It is clear from Fig.(3.1), a joint Bell state measurement of the  $b$  and  $c$  modes at 50 : 50 beam splitter and then directing the output modes of this beam splitter to polarization beam splitters (PBS); there are four alternatives  $c'_h$ ,  $c'_v$ ,  $b'_v$  and  $b'_h$  detections of photons at four detectors. The detection results of these detectors are denoted by  $qrst$ . Polarization beam splitters (PBS) reflect the vertical modes and transmit the horizontal modes. For photon number discriminating detectors  $qrst$  can indicate  $n_0 \in \mathbb{N}$   $\{\mathbb{N}$  are the natural numbers $\}$  and in case of threshold detectors they indicate *click*, *no-click*. Now the resultant mixed quantum state of the remaining modes  $a$  and  $d$  depending on the results of  $qrst$  detections after realistic Bell state measurement will be calculated. The Bayesian inference approach will help us to

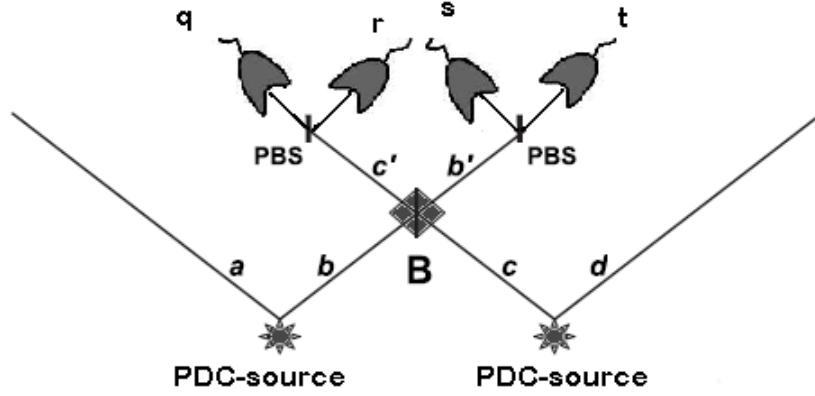


Figure 3.1: Entanglement swapping of photon-polarization qubits based on two PDC sources and a Bell-state measurement with four imperfect photon detectors. Four spatial modes are involved, labeled by  $a$ ,  $b$ ,  $c$ , and  $d$ . Two modes, one from the first and one from the second source,  $b$  and  $c$ , respectively, are combined at a balanced beam splitter (B). The exits of the latter, denoted by  $b'$  and  $c'$ , respectively, are directed to polarizing beam splitters (PBSs) and then detected at four detectors: one for the H and one for the V polarization of each of the  $c'$  and  $b'$  modes. The four detectors are inefficient photon detectors subject to dark counts. Their readout is denoted by  $(qrst)$ . Given this readout we are interested in the entangled quantum state of the remaining  $a$  and  $d$  modes depending on experimental parameters characterizing the deficiencies of the experiment.

calculate the probability  $P_{ijkl}^{qrst}$  of this state, where  $P(ijkl)$  is the probability of the hypothetical ideal Bell measurements corresponding to the resultant pure quantum state  $|\phi_{ijkl}\rangle$  of  $a$  and  $d$  modes. Thus the resultant quantum state of the remaining modes  $a$  and  $d$  after recording the actual read outs  $qrst$  with inefficient detectors will be

$$\rho^{qrst} = \sum_{ijkl} P_{ijkl}^{qrst} |\phi_{ijkl}\rangle \langle \phi_{ijkl}|. \quad (3.3.1)$$

Consider the quantum state generated by the two type-I PDC sources Eq.(2.5.19) which has been calculated earlier.

$$|\chi\rangle = \exp[4\omega(\chi)] \exp[\hat{a}_h^\dagger \hat{b}_h^\dagger + \hat{a}_v^\dagger \hat{b}_v^\dagger + \hat{c}_h^\dagger \hat{d}_h^\dagger + \hat{c}_v^\dagger \hat{d}_v^\dagger] |vac\rangle. \quad (3.3.2)$$

Suppose four detectors of the Bell measurement on  $b$  and  $c$  modes are perfect i.e  $\eta = 1$  and no dark counts. Now applying the balanced beam splitter transformation  $\begin{pmatrix} \hat{b}_h \\ \hat{c}_h \end{pmatrix} \rightarrow B^\dagger \begin{pmatrix} \hat{b}'_h \\ \hat{c}'_h \end{pmatrix}$ ,  $\begin{pmatrix} \hat{b}_h^\dagger \\ \hat{c}_h^\dagger \end{pmatrix} \rightarrow B^T \begin{pmatrix} \hat{b}'_h^\dagger \\ \hat{c}'_h^\dagger \end{pmatrix}$ , to get ideal read outs  $(ijkl)$  using rules [3] where

$$\hat{U} = \frac{1}{2} \begin{pmatrix} 1 & 1 \\ -1 & 1 \end{pmatrix}, \quad (3.3.3)$$

and similarly for vertical polarization. Now using the projection operator to project the resultant four mode quantum state on to the subspace corresponding to the projection operator

$$\hat{\prod}_{c'_h, c'_v, b'_v, b'_h}^{ijkl} := (|i\rangle\langle i|)_{c'_h} \otimes (|j\rangle\langle j|)_{c'_v} \otimes (|k\rangle\langle k|)_{b'_v} \otimes (|l\rangle\langle l|)_{b'_h} \quad (3.3.4)$$

$$\otimes I_{a_h} \otimes I_{a_v} \otimes I_{d_v} \otimes I_{d_h}.$$

The modes  $c'_h, c'_v, b'_v$  and  $b'_h$  are the output modes of the beam splitter.  $(|i\rangle\langle i|)_{c'_h}$  represents the projection operator corresponding to the Fock state  $|i\rangle$  of mode  $c'_h$  and similarly the others. The post measurement quantum state after applying the projection operator in Eq.(3.3.5) and using state normalization is:

$$\frac{\hat{\prod}_{c'_h, c'_v, b'_v, b'_h}^{ijkl} \hat{U}_B |\chi\rangle}{\| \hat{\prod}_{c'_h, c'_v, b'_v, b'_h}^{ijkl} \hat{U}_B |\chi\rangle \|} = |i^{c'_h} j^{c'_v} k^{b'_v} l^{b'_h}\rangle \otimes |\phi_{ijkl}\rangle. \quad (3.3.5)$$

where

$$|\phi_{ijkl}\rangle \equiv \frac{1}{\sqrt{i!j!k!l!}} \left( \frac{\hat{d}_h^\dagger - \hat{a}_h^\dagger}{\sqrt{2}} \right)^i \left( \frac{\hat{d}_v^\dagger - \hat{a}_v^\dagger}{\sqrt{2}} \right)^j \left( \frac{\hat{a}_v^\dagger + \hat{d}_v^\dagger}{\sqrt{2}} \right)^k \left( \frac{\hat{a}_h^\dagger + \hat{d}_h^\dagger}{\sqrt{2}} \right)^l |vac\rangle,$$

$$= \frac{1}{(\sqrt{2})^{i+j+k+l} \sqrt{i!j!k!l!}} \sum_{\mu=0}^i \sum_{\nu=0}^j \sum_{\kappa=0}^k \sum_{\lambda=0}^l (-1)^{\mu+\nu}$$

$$\times \binom{i}{\mu} \binom{j}{\nu} \binom{k}{\kappa} \binom{l}{\lambda}$$

$$\times (\hat{a}_h^\dagger)^{\mu+\lambda} (\hat{a}_v^\dagger)^{\nu+\kappa} (\hat{d}_h^\dagger)^{i+l-\mu-\lambda} (\hat{d}_v^\dagger)^{j+k+\nu+\kappa} |vac\rangle. \quad (3.3.6)$$

Now discarding the first factor in Eq.(3.3.5), as the Bell measurement is done on the  $b$  and  $c$  modes, so the photons in these modes will be destroyed after the measurement. The remaining factor  $|\phi_{ijkl}\rangle$  is the resultant pure state of the outgoing modes  $a$  and  $d$ . Hence the corresponding probability of the hypothetical ideal readout  $(ijkl)$  then will be

$$P(ijkl) = \| \hat{\prod}_{c'_h, c'_v, b'_v, b'_h}^{ijkl} \hat{U}_B |\chi\rangle \|^2 = \frac{[\tanh \chi]^{2(i+j+k+l)}}{\cosh^8 \chi}. \quad (3.3.7)$$

In an actual experiment, given an actual detector readout  $(qrst)$  of an imperfect Bell measurement with faulty photon number discriminating detectors having



dark count probability  $\rho_{dc}$ , One can not find the corresponding resultant postmeasurement quantum state for the modes a and d nor the probability of its occurrence. However using Bayesian theorem one can calculate the posterior probability  $P_{ijkl}^{qrst} := P(ijkl|qrst)$  of the hypothesis  $(ijkl)$  given that the event  $(qrst)$  has been obtained:

$$P_{ijkl}^{qrst} \equiv P(ijkl|qrst) = \frac{P(qrst|ijkl)P(ijkl)}{P(qrst)}, \quad (3.3.8)$$

$$P(ijkl|qrst) = \frac{P(qrst|ijkl)P(ijkl)}{\sum_{i',j',k',l'=0}^{\infty} P(qrst|i'j'k'l')P(i'j'k'l')}, \quad (3.3.9)$$

where,  $P(qrst|ijkl)$  is the conditional probability for obtaining the event  $(qrst)$  given that that the hypothesis or ideal  $(ijkl)$  event would have happened if the detectors used for Bell measurement had been ideal. Using this approach the required result Eq.(3.3.1) can be obtained.

Since the four detectors are statistically independent from one another, so the probabilities  $P(qrst|ijkl)$  factorize into four terms,

$$P_{\eta,\rho_{dc}}(qrst|ijkl) = P_{\eta,\rho_{dc}}(q|i)P_{\eta,\rho_{dc}}(r|j)P_{\eta,\rho_{dc}}(s|k)P_{\eta,\rho_{dc}}(t|l), \quad (3.3.10)$$

where each of these probabilities has been calculated as in Eq.(2.8.22). Now combining these factors with Eq.(3.3.7) implies a factorization of the posterior probability given in Eq.(3.3.1). So,

$$P_{ijkl}^{qrst}(\chi, \eta, \rho_{dc}) = f_i^q(\chi, \eta, \rho_{dc})f_j^r(\chi, \eta, \rho_{dc}) \times f_k^s(\chi, \eta, \rho_{dc})f_l^t(\chi, \eta, \rho_{dc}). \quad (3.3.11)$$

Now using Eq.(3.3.7) and the physical assumption considered in Eq.(3.3.11) into Eq.(3.3.1), we get

$$f_i^q(\chi, \eta, \rho_{dc}) \equiv \frac{P_{\eta,\rho_{dc}}(q|i) \tanh^{2i}(\chi)}{\sum_{i'=0}^{\infty} P_{\eta,\rho_{dc}}(q|i') \tanh^{2i'}(\chi)}. \quad (3.3.12)$$

Finally inserting the Eq.(2.8.22) into Eq.(3.3.12) we will get the following form of  $f_i^q(\chi, \eta, \rho_{dc})$ ,

$$f_i^q(\chi, \eta, \rho_{dc}) = \frac{\frac{(1-\eta)(1-\rho_{dc})}{1-\eta(1-\rho_{dc})} \left(\frac{\eta}{1-\eta}\right)^q \Omega(i, q; \eta, \rho_{dc}) \tanh^{2i}(\chi)}{\sum_{i'=0}^{\infty} P_{\eta,\rho_{dc}}(q|i') \tanh^{2i'}(\chi)}, \quad (3.3.13)$$

where

$$P_{\eta, \rho_{dc}}(q|i) \tanh^{2i'}(\chi) = \sum_{i'=q}^{\infty} P_{\eta, \rho_{dc}}(q|i) \tanh^{2i'}(\chi) + \sum_{i'=q+1}^{\infty} P_{\eta, \rho_{dc}}(q|i) \tanh^{2i'}(\chi),$$

$$\text{for } i' = 0 \rightarrow q \quad i \leq q \quad \text{or} \quad q \leq i$$

$$\text{for } i' = q + 1 \rightarrow \infty \quad i > q$$

$$\begin{aligned} \sum_{i'=0}^{\infty} P_{\eta, \rho_{dc}}(q|i) \tanh^{2i'}(\chi) &= \sum_{i'=0}^{\infty} \frac{(1-\eta)(1-\rho_{dc})}{1-\eta(1-\rho_{dc})} \left[ \frac{1-\eta}{\eta} b(\eta, \rho_{dc}) \right]^{q-i} \eta^{i'} G(q, i; \eta, \rho_{dc}) \\ &+ \sum_{i'=0}^{\infty} \frac{(1-\eta)(1-\rho_{dc})}{1-\eta(1-\rho_{dc})} \left( \frac{\eta}{1-\eta} \right)^q (1-\eta)^{i'} \\ &G(i, q; \eta, \rho_{dc}). \end{aligned} \quad (3.3.14)$$

After putting this expression back in Eq.(3.3.13) and doing some simple algebra, final expression will be:

$$f_i^q(\chi, \eta, \rho_{dc}) = \begin{cases} \frac{\tanh^{2i} \chi (1-\eta)^{i-q} \Omega(i, q; \eta, \rho_{dc})}{g(q; \chi, \eta, \rho_{dc})} & \text{if } i \geq q \\ \frac{\tanh^{2i} \chi \eta^{2(i-q)} (1-\eta)^{q-i} [b(\eta, \rho_{dc})]^{q-i} \Omega(q, i; \eta, \rho_{dc})}{g(q; \chi, \eta, \rho_{dc})} & \text{if } q \geq i, \end{cases} \quad (3.3.15)$$

where

$$\begin{aligned} g(q; \chi, \eta, \rho_{dc}) &= \sum_{i'=0}^q \tanh^{2i'}(\chi) \eta^{2(i'-q)} (1-\eta)^{q-i'} [b(\eta, \rho_{dc})]^{q-i'} \Omega(q, i'; \eta, \rho_{dc}) \\ &+ \sum_{i'=q+1}^{\infty} \tanh^{2i'}(\chi) (1-\eta)^{i'-q} \Omega(i', q; \eta, \rho_{dc}). \end{aligned} \quad (3.3.16)$$

Similarly the other expressions  $f_j^r(\chi, \eta, \rho_{dc})$ ,  $f_k^s(\chi, \eta, \rho_{dc})$ ,  $f_l^t(\chi, \eta, \rho_{dc})$  present in Eq.(3.3.11) can be calculated. Thus Eq.(3.3.11), Eq.(3.3.15), Eq.(3.3.16) are used to calculate the result for photon number discriminating detectors. The mixed quantum state of the remaining modes a and d after an imperfect Bell measurement result  $qrst$  can be easily calculated using photon number discriminating detectors with efficiency  $\eta$  and dark count probability  $\rho_{dc}$  as we now know the probabilities  $P_{ijkl}^{qrst}$  for all possible hypothetical readouts  $ijkl$ .

As discussed earlier that photon number discriminating detectors are still a technological challenge, so for a more realistic and practical situation we consider threshold detectors. In the case of threshold detectors the events  $qrst$  of the Bell measurement consists of readouts  $q, r, s, t \in \text{click}, \text{no-click}$ . The conditional probabilities

for these kind of detectors are given in Eq.(2.8.26) and Eq.(2.8.27) in the last chapter. So the functions given in Eq.(3.3.11) can be easily calculated using Eq.(3.3.13), the result will be

$$f_i^{no-click}(\chi, \eta, \rho_{dc}) = [h(\chi, \eta, \rho_{dc})]^i [1 - h(\chi, \eta, \rho_{dc})], \quad (3.3.17)$$

$$f_i^{click}(\chi, \eta, \rho_{dc}) = \frac{\tanh^{2i} \chi - (1 - \rho_{dc})[h(\chi, \eta, \rho_{dc})]^i}{\cosh^2 \chi - \frac{1 - \rho_{dc}}{1 - h(\chi, \eta, \rho_{dc})}}, \quad (3.3.18)$$

where  $h(\chi, \eta, \rho_{dc})$  is given as,

$$h(\chi, \eta, \rho_{dc}) := [1 - \eta(1 - \rho_{dc})] \tanh^{2i} \chi. \quad (3.3.19)$$

For threshold detectors, the posterior probabilities can be found by using Eq.(3.3.11) together with Eq.(3.3.17) and Eq.(3.3.19).

Bayesian reasoning and the physical assumption that the four detectors of the Bell measurement are statistically independent as given in Eq.(3.3.10) (are used to derive the resultant quantum state Eq.(3.3.1) of the remaining modes  $a$  and  $d$ ). It was assumed earlier that all the four detectors have same efficiency  $\eta$  but we can now generalize the results for different efficiencies as well as different dark count probabilities for four detectors. The derivation is very simple and the result reads

$$P_{ijkl}^{qrst}(\chi, \{\eta_\nu\}, \{\rho_{dc\nu}\}) = f_i^q(\chi, \eta_1, \rho_{dc1}) f_j^r(\chi, \eta_2, \rho_{dc2}) \times f_k^s(\chi, \eta_3, \rho_{dc3}) f_l^t(\chi, \eta_4, \rho_{dc4}), \quad (3.3.20)$$

where  $\eta_\nu$  and  $\rho_{dc\nu}$ ,  $\nu = 1, 2, 3, 4$  are arbitrary and in general different efficiencies and dark count probabilities of the four detectors.

### 3.4 Comparison with Experimental Swapping

In the last section the theory for experimental entanglement swapping is completely explained. Now to test the validity of the theory it is tested against the results of real entanglement experiments [3]. Entanglement verification in these experiments is accomplished by measuring certain correlation coefficients for polarization related to the CHSH (Clauser-Horne-Shimony-Holt) Bell inequality [32], obtained via variable

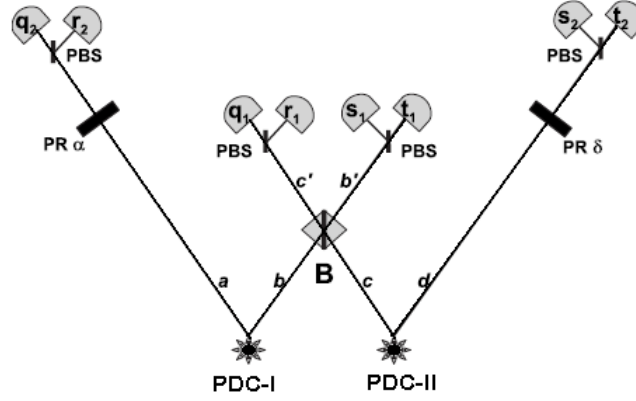


Figure 3.2: Scheme for entanglement verification in an entanglement swapping experiment. A Bell state measurement with imperfect threshold detectors is performed on the  $c$  and  $b$  modes. A readout  $(q_1 r_1 s_1 t_1)$  is recorded. Polarization rotators (PRs) parameterized by angles  $\alpha$  and  $\delta$  are applied to the remaining  $a$  and  $d$  modes prior to polarization measurements using polarizing beam splitters (PBSs) and non ideal threshold detectors. The readout of the second measurement is denoted by  $(q_2 r_2 s_2 t_2)$ .

polarization directions of analyzers placed in front of the detectors used for  $a$  and  $d$  modes as shown in Fig.(3.2).

Now to simulate a fourfold coincidence experiment as given is [3] we proceed as follows. As described earlier, we will compare our theory with the experimental situations given in [4, 31]. So we consider the fourfold coincidence events in which the Bell measurement on  $b$  and  $c$  modes corresponds in the ideal case scenario to a projection onto the Bell state

$$|\psi^-\rangle_{cb} = \frac{1}{\sqrt{2}}(\hat{c}_h^\dagger \hat{b}_v^\dagger - \hat{c}_v^\dagger \hat{b}_h^\dagger)|vac\rangle, \quad (3.4.1)$$

So its clear that after applying projection postulate, the remaining modes  $a$  and  $d$  are also left in the same Bell state i.e  $|\psi^-\rangle_{ad}$ .

Let us for a moment consider that our sources and detectors are ideal then, a projection to Bell state is achieved whenever there are coincidence clicks of the two detectors for  $c_h$  and  $b_v$  and vice versa. For this we can exploit the fact that the Bell state  $|\psi^-\rangle_{cb}$  is antisymmetric under the exchange of labels  $c$  and  $b$  using fermionic statistics, which means the two photons have to emerge from different output ports

of the beam splitter as shown in Fig.(3.2). The remaining three Bell states  $|\phi^+\rangle, |\psi^\pm\rangle$  are symmetric under the exchange of labels c and b implying bosonic statistics, means that photons will emerge from the same output port of the beam splitter. Hence, for the assumption of ideal sources and detectors, observing coincidence clicks on both sides of the beam splitter is an experimental evidence for a projection onto the state  $|\psi^-\rangle_{cb}$  and thus also the existence of the state  $|\psi^-\rangle_{ad}$  for  $a$  and  $d$  modes. For the assumption of antisymmetric state  $|\psi^-\rangle_{cb}$  to be satisfied, only the coincidence clicks of “ $c_h$  and  $b_v$ ” or “ $c_v$ ” and “ $b_h$ ” are possible, but not of the clicks of the same polarization.

As in the real experimental scenario, the PDC sources and detectors are not ideal. So, due to the presence of different inefficiencies, the actual quantum state after suggested Bell state measurement will deviate from  $|\psi^-\rangle_{ad}$ . More specifically, even if the detectors used for the Bell measurement were ideal ( $\eta = 1, \rho_{dc} = 0$ ), they would never indicate a projection onto  $|\psi^-\rangle_{cb}$  and thus also prepare the Bell state  $|\psi^-\rangle_{ad}$  unless the photon pair sources were ideal. The reason behind this issue is the multipair nature of the PDC sources which precludes a projection onto the Bell state  $|\psi^-\rangle_{cb}$  independent of the quality of the detectors used. To illustrate this fact, let us consider the case of ideal photon number discriminating detectors and the outcome of the Bell measurement on  $b$  and  $c$  modes on these detectors is  $(1, 0, 1, 0)$ . As it is assumed that the detectors are ideal photon number discriminating detectors so by taking  $\eta \rightarrow 1$ , we have

$$\lim_{\eta \rightarrow 1} f_i^q(\chi, \eta, \rho_{dc} = 0) = \delta_{qi},$$

where  $\delta_{qi}$  is the kronecker delta function. This is exactly what one should expect in the case of ideal detectors with no dark counts. Thus, in the situation described above, we have  $F_{ijkl}^{qrst} = \delta_{qi}\delta_{rj}\delta_{sk}\delta_{tl}$  and the state in Eq.(3.3.1) reduces to a single component, the pure state  $|\phi_{1010}\rangle$  as,

$$|\phi_{ijkl}\rangle = \frac{1}{(\sqrt{2})^{i+j+k+l} \sqrt{i!j!k!l!}} \sum_{\mu=0}^i \sum_{\nu=0}^j \sum_{\kappa=0}^k \sum_{\lambda=0}^l (-1)^{\mu+\nu} \begin{pmatrix} i \\ \mu \end{pmatrix} \begin{pmatrix} j \\ \nu \end{pmatrix} \begin{pmatrix} k \\ \kappa \end{pmatrix} \begin{pmatrix} l \\ \lambda \end{pmatrix} (\hat{a}_h^\dagger)^{\mu+\lambda} (\hat{a}_v^\dagger)^{\nu+\kappa} (\hat{d}_h^\dagger)^{i+l-\mu-\lambda} (\hat{d}_v^\dagger)^{j+k-\nu-\kappa} |0000\rangle,$$

$$\begin{aligned}
|\phi_{1010}\rangle &= \frac{1}{2} \begin{pmatrix} 1 \\ 0 \end{pmatrix} \begin{pmatrix} 0 \\ 0 \end{pmatrix} \begin{pmatrix} 1 \\ 0 \end{pmatrix} \begin{pmatrix} 0 \\ 0 \end{pmatrix} (\hat{a}_h^\dagger)^0 (\hat{a}_v^\dagger)^0 (\hat{d}_h^\dagger)^1 (\hat{d}_v^\dagger)^1 |0000\rangle \\
&+ \frac{1}{2} \begin{pmatrix} 1 \\ 0 \end{pmatrix} \begin{pmatrix} 0 \\ 0 \end{pmatrix} \begin{pmatrix} 1 \\ 1 \end{pmatrix} \begin{pmatrix} 0 \\ 0 \end{pmatrix} (\hat{a}_h^\dagger)^0 (\hat{a}_v^\dagger)^1 (\hat{d}_h^\dagger)^1 (\hat{d}_v^\dagger)^0 |0000\rangle \\
&- \frac{1}{2} \begin{pmatrix} 1 \\ 1 \end{pmatrix} \begin{pmatrix} 0 \\ 0 \end{pmatrix} \begin{pmatrix} 1 \\ 0 \end{pmatrix} \begin{pmatrix} 0 \\ 0 \end{pmatrix} (\hat{a}_h^\dagger)^1 (\hat{a}_v^\dagger)^0 (\hat{d}_h^\dagger)^0 (\hat{d}_v^\dagger)^1 |0000\rangle \\
&- \frac{1}{2} \begin{pmatrix} 1 \\ 1 \end{pmatrix} \begin{pmatrix} 0 \\ 0 \end{pmatrix} \begin{pmatrix} 1 \\ 1 \end{pmatrix} \begin{pmatrix} 0 \\ 0 \end{pmatrix} (\hat{a}_h^\dagger)^1 (\hat{a}_v^\dagger)^1 (\hat{d}_h^\dagger)^0 (\hat{d}_v^\dagger)^0 |0000\rangle \\
&= \frac{1}{2} [\hat{d}_h^\dagger \hat{d}_v^\dagger |0000\rangle + \hat{a}_v^\dagger \hat{d}_h^\dagger |0000\rangle - \hat{a}_h^\dagger \hat{d}_v^\dagger |0000\rangle - \hat{a}_h^\dagger \hat{a}_v^\dagger |0000\rangle], \\
&= \frac{1}{2} [|0011\rangle + |0101\rangle - |1010\rangle - |1100\rangle], \\
|\phi_{1010}\rangle &= \frac{1}{\sqrt{2}} \left[ \frac{|0011\rangle - |1100\rangle}{\sqrt{2}} + \frac{|0101\rangle - |1010\rangle}{\sqrt{2}} \right]. \tag{3.4.2}
\end{aligned}$$

Thus apart from the expected Bell state  $|\psi\rangle_{cb}$ , we get another term which is the superposition of the two photons either in  $a$  mode and no photon in  $d$  mode or vice versa. Hence the entanglement swapping performed with PDC sources cannot produce a perfect projection onto the state  $|\psi\rangle_{cb}$  even if the detectors used for the Bell measurement are perfectly ideal.

In case of imperfect threshold detectors which is being discussed here, a projection onto the Bell state  $|\psi^-\rangle_{cb}$  is achieved whenever one of the following non-ideal Bell measurement events  $q, r, s, t$  is obtained:  $(1, 0, 1, 0)$  or  $(0, 1, 0, 1)$  where  $q = 1$  means a click and  $q = 0$  means detectors does not click.

The setup used for entanglement swapping via fourfold coincidence measurement is very similar to the one described in [4]. It is illustrated in Fig.(3.2). To vary the polarization of  $a$  and  $d$  modes, polarization rotators are introduced into their spatial paths prior to polarization beam splitters. The polarizations of  $a$  and  $d$  can be varied independently by varying angles  $\alpha$  and  $\delta$ . To avoid any confusion, let us get cleared that  $\alpha$  and  $\delta$  stands for the rotation angles of polarization vectors in the real space and not of the Bloch vectors on the Bloch sphere. Neither do they mean rotation angles of  $\lambda/2$  plates which are used in the actual experiment to cause polarization rotations.

Polarization rotators prior to PBS are used to separate horizontal and vertical polarizations. The absolute angle of rotation in each modes determines the basis of the polarization measurement. In the ideal case scenario, the polarization correlations should depend on the relative angle only between two polarization rotators. The choice of rotation of polarization is quite independent. For the purpose here the polarization of mode  $a$  is chosen by a fixed angle  $\alpha = \pi/4$  and the probabilities for coincidence clicks of the detectors click for measurement on  $a$  and  $d$  modes are calculated numerically for different angles of polarization rotation of the  $d$  mode i.e by varying  $\delta$ . Here, as it has been explained earlier that the results of the Bell measurement on  $b$  and  $c$  modes will be  $(1, 0, 1, 0)$  or  $(0, 1, 0, 1)$ . The four detectors for the measurement on  $a$  and  $d$  modes are denoted by  $D_a^+$ ,  $D_a^-$  and  $D_d^+$ ,  $D_d^-$  corresponding to analyzing the  $a$  mode along the  $+45^\circ$  and  $-45^\circ$  axes and the  $d$  mode along the variable polarization from  $-\delta$  to  $+\delta$  respectively. The four-tuple events  $(q_2, r_2, s_2, t_2)$  of the measurements on  $a$  and  $d$  mods corresponds to the readouts of the four detectors  $(D_a^+, D_a^-, D_d^+, D_d^-)$ .

In what follows, the probability for fourfold coincidence using the scheme explained above for experimental entanglement swapping is calculated. The polarization rotators acting on  $a$  and  $d$  modes can be represented by the unitary operators

$$\hat{U}(\tilde{\alpha}) = \exp[i\tilde{\alpha}\hat{J}_a], \quad (3.4.3)$$

$$\hat{U}(\tilde{\delta}) = \exp[i\tilde{\delta}\hat{J}_d], \quad (3.4.4)$$

with  $\tilde{\delta}, \tilde{\alpha} \in R$  and  $\tilde{\alpha} = 2\alpha, \tilde{\delta} = 2\delta$  where  $\alpha$  and  $\delta$  are the are polarization vectors in the real space. The generators of rotation

$$\hat{J}_a := \frac{1}{2}(\hat{a}_v^\dagger \hat{a}_h^\dagger + \hat{a}_v \hat{a}_h), \quad (3.4.5)$$

$$\hat{J}_d := \frac{1}{2}(\hat{d}_v^\dagger \hat{d}_h^\dagger + \hat{d}_v \hat{d}_h). \quad (3.4.6)$$

If the detectors had been ideal then the conditional probability that the polarization measurement on  $a$  and  $d$  modes would have yielded the result  $(i_2, j_2, k_2, l_2)$  if an imperfect Bell measurement on  $b$  and  $c$  modes had given an event  $(q_1, r_1, s_1, t_1)$ ,

is given by

$$\begin{aligned}
P(i_2 j_2 k_2 l_2 | q_1 r_1 s_1 t_1) &= \text{Tr}\{(|i_2^{a_h} j_2^{a_v} k_2^{d_v} l_2^{d_h}\rangle \langle i_2^{a_h} j_2^{a_v} k_2^{d_v} l_2^{d_h}|) \\
&\quad [\hat{U}_a(\tilde{\alpha}) \otimes \hat{U}_d(\tilde{\delta}) \rho^{q_1 r_1 s_1 t_1} \hat{U}_a^\dagger(\tilde{\alpha}) \otimes \hat{U}_d^\dagger(\tilde{\delta})]\}, \\
&= \sum_{i_1 j_1 k_1 l_1} W_{i_2 j_2 k_2 l_2}^{i_1 j_1 k_1 l_1}(\tilde{\alpha}, \tilde{\delta}) P_{i_1 j_1 k_1 l_1}^{q_1 r_1 s_1 t_1}(\chi, \{\eta_\nu^{(1)}\}, \{\rho_{d\nu}^{(1)}\}), \tag{3.4.7}
\end{aligned}$$

where Eq.(3.3.1) is used and the transition probabilities

$$W_{i_2 j_2 k_2 l_2}^{i_1 j_1 k_1 l_1}(\tilde{\alpha}, \tilde{\delta}) := |\langle i_2^{a_h} j_2^{a_v} k_2^{d_v} l_2^{d_h} | \hat{U}_a(\tilde{\alpha}) \otimes \hat{U}_d(\tilde{\delta}) | \phi_{i_1 j_1 k_1 l_1} \rangle|^2, \tag{3.4.8}$$

are introduced.

For numerical simulations, this transition probability can be calculated as,

$$\hat{U}_a(\tilde{\alpha}) = \frac{i\tilde{\alpha}}{2} [\hat{a}_v^\dagger \hat{a}_h^\dagger + \hat{a}_v \hat{a}_h], \tag{3.4.9}$$

$$\hat{U}_d(\tilde{\alpha}) = \frac{i\tilde{\delta}}{2} [\hat{d}_v^\dagger \hat{d}_h^\dagger + \hat{d}_v \hat{d}_h]. \tag{3.4.10}$$

Using Baker-Campbell-Hausdorff formula one can find the explicit expression for  $W_{i_2 j_2 k_2 l_2}^{i_1 j_1 k_1 l_1}(\tilde{\alpha}, \tilde{\delta})$  easily. Let us define

$$\hat{S}_+ := \hat{a}_v^\dagger \hat{a}_h, \quad \hat{S}_- := \hat{a}_v \hat{a}_h^\dagger, \quad \hat{S}_z := \frac{1}{2} (\hat{a}_v^\dagger \hat{a}_v - \hat{a}_h^\dagger \hat{a}_h). \tag{3.4.11}$$

These operators are the bosonic representation of  $SU(2)$  Lie algebra. According to [3], the following composition formulas are used to solve disentangle the exponential functions of the generators on the  $SU(2)$  Lie algebra.

$$\exp[i\tilde{\alpha}(\theta_+ \hat{S}_+ + \theta_z \hat{S}_z + \theta_- \hat{S}_-)] = \exp[f_+(\tilde{\alpha}) \hat{S}_+] \exp[f_z(\tilde{\alpha}) \hat{S}_z] \exp[f_-(\tilde{\alpha}) \hat{S}_-], \tag{3.4.12}$$

where the functions  $f_\pm(\tilde{\alpha}), f_z(\tilde{\alpha})$  are defined as

$$f_\pm(\tilde{\alpha}) := \frac{i\theta_\pm}{\Gamma_1} \frac{\sin(\Gamma_1 \tilde{\alpha})}{\cos(\Gamma_1 \tilde{\alpha}) - i\theta_z \sin(\Gamma_1 \tilde{\alpha}) / (2\Gamma_1)},$$

$$f_z(\tilde{\alpha}) := -2 \ln[\cos(\Gamma_1 \tilde{\alpha}) - i \frac{\theta_z}{2\Gamma_1} \sin(\Gamma_1 \tilde{\alpha})],$$

with

$$\Gamma_1^2 := \theta_+ \theta_- + \frac{\theta_z^2}{4}.$$



Now using this decomposition formula to Eq.(3.4.9) and in present case  $\theta_+ = \theta_- = 1/2$ ,  $\theta_z = 1/2$ , and

$$f_{\pm}(\tilde{\alpha}) = i \tan \frac{\tilde{\alpha}}{2},$$

$$f_z(\tilde{\alpha}) = -2 \ln(\cos \frac{\tilde{\alpha}}{2}).$$

Thus, Eq.(3.4.9) becomes

$$\begin{aligned} \hat{U}_a(\tilde{\alpha}) &= \exp[i \tan(\frac{\tilde{\alpha}}{2}) \hat{a}_v^\dagger \hat{a}_h] \exp[-\ln(\cos \frac{\tilde{\alpha}}{2}) \hat{a}_v^\dagger \hat{a}_v] \\ &\times \exp[\ln(\cos \frac{\tilde{\alpha}}{2}) \hat{a}_h^\dagger \hat{a}_h] \exp[i \tan(\frac{\tilde{\alpha}}{2}) \hat{a}_v \hat{a}_h^\dagger] \end{aligned} \quad (3.4.13)$$

In the similar way one obtains a decomposed form of  $\hat{U}_d(\tilde{\delta})$  in Eq.(3.4.10) as

$$\begin{aligned} \hat{U}_d(\tilde{\delta}) &= \exp[i \tan(\frac{\tilde{\delta}}{2}) \hat{d}_v^\dagger \hat{d}_h] \exp[-\ln(\cos \frac{\tilde{\delta}}{2}) \hat{d}_v^\dagger \hat{d}_v] \\ &\times \exp[\ln(\cos \frac{\tilde{\delta}}{2}) \hat{d}_h^\dagger \hat{d}_h] \exp[i \tan(\frac{\tilde{\delta}}{2}) \hat{d}_v \hat{d}_h^\dagger] \end{aligned} \quad (3.4.14)$$

After using these expressions in Eq.(3.4.8) to derive the transition probabilities. The result reads

$$W_{i_2 j_2 k_2 l_2}^{i_1 j_1 k_1 l_1}(\tilde{\alpha}, \tilde{\delta}) = |A_{i_2 j_2 k_2 l_2}^{i_1 j_1 k_2 l_1}(\tilde{\alpha}, \tilde{\delta})|^2 \quad (3.4.15)$$

with

$$A_{i_2 j_2 k_2 l_2}^{i_1 j_1 k_2 l_1}(\tilde{\alpha}, \tilde{\delta}) := |\langle i_2^{a_h} j_2^{a_v} k_2^{d_v} l_2^{d_h} | \hat{U}_a(\tilde{\alpha}) \otimes \hat{U}_d(\tilde{\delta}) | \phi_{i_1 j_1 k_1 l_1} \rangle| \quad (3.4.16)$$

$$\begin{aligned} A_{i_2 j_2 k_2 l_2}^{i_1 j_1 k_2 l_1}(\tilde{\alpha}, \tilde{\delta}) &= \frac{1}{(\sqrt{2})^{i_1+j_1+k_1+l_1} \sqrt{i_1! j_1! k_1! l_1!}} \sum_{\mu=0}^{i_1} \sum_{\nu=0}^{j_1} \sum_{\kappa=0}^{k_1} \sum_{\lambda=0}^{l_1} \sum_{n_a=0}^{\min\{j_2, \nu+\kappa\}} \sum_{n_d=0}^{\min\{k_2, j_1+k_1-\nu+\kappa\}} (-1)^{\mu+\nu} \\ &\times \binom{i_1}{\mu} \binom{j_1}{\nu} \binom{k_1}{\kappa} \binom{l_1}{\lambda} \delta_{\mu+\nu+\kappa+\lambda, i_2+j_2} \delta_{i_1+j_1+k_1+l_1, i_2+j_2+k_2+l_2} \\ &\times \sqrt{(\mu+\lambda)! (\nu+\kappa)! (i_1+l_1-\mu-\lambda)! (j_1+k_1-\nu-\kappa)!} [\cos \frac{\tilde{\alpha}}{2}]^{i_2+j_2-2n_a} \\ &\times [\cos \frac{\tilde{\delta}}{2}]^{k_2+l_2-2n_d} \left\{ \frac{[i \tan \frac{\tilde{\alpha}}{2}]^{j_2+\nu+\kappa-2n_a} [i \tan \frac{\tilde{\alpha}}{2}]^{k_2+j_1+k_1-\nu-\kappa-2n_d}}{(j_2-n_a)! (\nu+\kappa-n_a)! (k_2-n_d)! (j_1+k_1-\nu-\kappa-n_d)} \right\} \\ &\times [\prod_{m_1=1}^{j_2-n_a} (n_a+m_1)]^{1/2} [\prod_{m_2=1}^{\nu+\kappa-n_a} (n_a+m_2)]^{1/2} [\prod_{m_3=1}^{j_2-n_a} (i_2+m_3)]^{1/2} \\ &\times [\prod_{m_4=1}^{\nu+\kappa-n_a} (i_2+j_2-\nu-\kappa+m_4)]^{1/2} [\prod_{m_5=1}^{k_2-n_d} (n_d+m_5)]^{1/2} \\ &\times [\prod_{m_6=1}^{j_1+k_1-\nu-\kappa-n_d} (n_d+m_6)]^{1/2} [\prod_{m_7=1}^{k_2-n_d} (l_2+m_7)]^{1/2} \\ &\times [\prod_{m_8=1}^{j_1+k_1-\nu-\kappa-n_d} (k_2+l_2-j_1-k_1+\nu+\kappa+m_8)]^{1/2}, \end{aligned} \quad (3.4.17)$$

Given an event  $(q_1 r_1 s_1 t_1)$  of a nonideal Bell measurement on modes  $b$  and  $c$ , the conditional probability to observe the event  $(q_2 r_2 s_2 t_2)$  with nonideal imperfect detectors is denoted and calculated as

$$\begin{aligned}
Q_{q_2 r_2 s_2 t_2}^{q_1 r_1 s_1 t_1}(\chi, \{\eta_\nu^{(1)}\}, \{\eta_\nu^{(2)}\}, \{\rho_{dc\nu}^{(1)}\}, \{\rho_{dc\nu}^{(2)}\}, \tilde{\alpha}, \tilde{\delta}) &:= \text{prob}(q_2 r_2 s_2 t_2 | q_1 r_1 s_1 t_1), \\
&= \sum_{i_2 j_2 k_2 l_2} \text{prob}(q_2 r_2 s_2 t_2 | q_1 r_1 s_1 t_1) \text{prob}(i_2 j_2 k_2 l_2 | q_1 r_1 s_1 t_1), \\
&= \sum_{i_2 j_2 k_2 l_2} P_{\eta_1^{(2)}, \rho_{dc1}^{(2)}}(q_2 | i_2) P_{\eta_2^{(2)}, \rho_{dc2}^{(2)}}(r_2 | j_2) \\
&\quad \times P_{\eta_3^{(2)}, \rho_{dc3}^{(2)}}(s_2 | k_2) P_{\eta_4^{(2)}, \rho_{dc4}^{(2)}}(t_2 | l_2) \\
&\quad \times \left( \sum_{i_1 j_1 k_1 l_1} W_{i_2 j_2 k_2 l_2}^{i_1 j_1 k_1 l_1}(\tilde{\alpha}, \tilde{\delta}) P_{i_1 j_1 k_1 l_1}^{q_1 r_1 s_1 t_1}(\chi, \{\eta_\nu^{(1)}\}, \{\rho_{dc\nu}^{(1)}\}) \right), \\
&= \sum_{i_2 j_2 k_2 l_2=0}^{\infty} \sum_{i_1 j_1 k_1 l_1=0}^{\infty} P_{\eta_1^{(2)}, \rho_{dc1}^{(2)}}(q_2 | i_2) P_{\eta_2^{(2)}, \rho_{dc2}^{(2)}}(r_2 | j_2) \\
&\quad \times P_{\eta_3^{(2)}, \rho_{dc3}^{(2)}}(s_2 | k_2) P_{\eta_4^{(2)}, \rho_{dc4}^{(2)}}(t_2 | l_2) \\
&\quad \times W_{i_2 j_2 k_2 l_2}^{i_1 j_1 k_1 l_1}(\tilde{\alpha}, \tilde{\delta}) P_{i_1 j_1 k_1 l_1}^{q_1 r_1 s_1 t_1}(\chi, \{\eta_\nu^{(1)}\}, \{\rho_{dc\nu}^{(1)}\}). \tag{3.4.18}
\end{aligned}$$

Now combining this result together with Eq.(3.3.11), Eq.(3.3.17) and Eq.(3.3.18), the four fold coincidence probability can be calculated numerically. As it is explained earlier that one conditioned on obtaining the readout  $(1_{c'_h}, 0_{c'_v}, 1_{b'_v}, 1_{b'_h})$  or  $(0_{c'_h}, 1_{c'_v}, 0_{b'_v}, 1_{b'_h})$  in the Bell measurement. Regardless which of the two events is given, the conditional probabilities of recording the events  $(1, 0, 1, 0)$ ,  $(0, 1, 1, 0)$ ,  $(0, 1, 0, 1)$  or  $(1, 0, 0, 1)$  can be calculated, using four imperfect threshold detectors  $(D_a^+, D_a^-, D_d^+, D_d^-)$  in the polarization measurement on  $a$  and  $d$  modes, depending on the varying angle of rotation of  $\delta$ .

# Chapter 4

## Theoretical Model for Experimental Dense Coding

### 4.1 Introduction

Quantum dense coding is a process or a technique used in quantum information to send two classical bits of information using only one qubit, with the aid of entanglement. In classical coding, a single-photon can convey only one of the two messages, or one bit of information per photon. In dense coding, a single-photon can convey one of the four messages, or two bits of information. Dense coding is possible because of the properties of photons (i.e polarization, spin, momentum) can be linked together through a particular process called quantum entanglement. It is a process that can link two photons even if they are located light years apart.

Suppose Alice would like to send classical information to Bob. She wants to send information through qubits instead of classical bits. Alice would encode the information in a qubit and send it to Bob. Bob recovers the information through some measurement after receiving the qubit from Alice. Then the question arises: how much classical information can be conveyed per qubit? Since nonorthogonal states cannot be distinguished properly, one would guess that Alice can do no better than one classical bit per qubit. Thus there is no advantage in using qubits instead of classical bits. However, with the additional assumption that the qubits in Alice

and Bob's possession are entangled, two classical bits per qubit can be achieved. The term *quantum dense coding* refers to this doubling of efficiency.

Dense coding is a method that increases the rate at which information may be sent through a noiseless quantum channel utilizing quantum entanglement. By sending a single qubit through a noiseless quantum channel between two parties gives a maximum rate of communication of one bit per qubit. If the sender's qubit is maximally entangled with receiver's qubit, then the process of dense coding increases the maximum rate of two bits per qubit.

As has been explained earlier, through the process of parametric down-conversion (PDC) in a pair of nonlinear crystals, a pair of photons gets entangled in polarization. Then a message which is to be sent is encoded in the polarization state by applying phase shifter with a pair of liquid crystal. Then the receiver will have to do some measurement on that state to decode that information. In this chapter we will discuss the theoretical model of experimental dense coding by taking into account all the inefficiencies present in different components of experimental setup.

## 4.2 Quantum Dense Coding

In quantum information theory qubits can be used to store and transmit information. Classical bit strings of the form 10010(*say*) can be sent using qubits prepared in the state  $|10010\rangle$ . The receiver can extract the information by measuring each qubit in the basis of  $|0\rangle, |1\rangle$  (i.e these are the eigenstates of measured observable). This measurement result yields the classical bit string with no ambiguity.

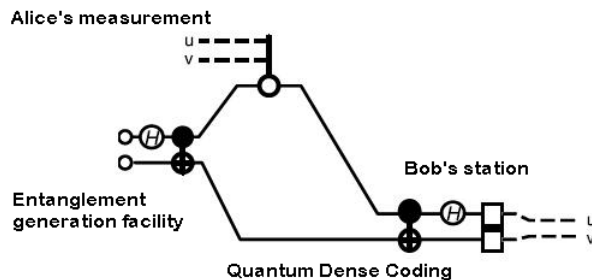


Figure 4.1: Theoretical Quantum Dense Coding.

Suppose now that Alice and Bob share an entangled pair of qubits, in the state  $|00\rangle + |11\rangle$  (this is a normalized maximally entangled Bell state but the normalization factor  $1/\sqrt{2}$  has been dropped to keep the notation simple). We assume a central mechanical facility generating the entangled pairs and sending one qubit to each of Alice and Bob, who have never communicated in the past. Using this entangled qubit in her possession, Alice can communicate two classical bits by sending Bob only one qubit. This idea due to Wiesner [6] is called “dense coding”, since only one qubit travels from Alice to Bob in order to convey the information of two classical bits. Here two qubits are actually involved but Alice can see only one of them in her possession. This method relies on the fact that four mutually orthogonal Bell states can be generated from each other by using operations on the single qubit. Suppose Alice wants to send the classical bit string of 00, 11, 10, 01 then she will start from the state  $|\psi\rangle = |00\rangle + |11\rangle$ . As mentioned earlier, Alice can generate any of the Bell basis states by operating on her qubit with one of the operators  $(I, X, Y, Z)$ . So, if Alice wants to send the classical bit string of 00 then she will leave her qubit unchanged. If Alice applies bit flip operation ( $X$ ) on her qubit the state will be

$$(X \otimes I)|\psi\rangle = |10\rangle + |01\rangle.$$

If she applies phase flip operation ( $Z$ ) instead of ( $X$ ) then

$$(Z \otimes I)|\psi\rangle = |00\rangle - |11\rangle.$$

Finally if she does both bit flip and phase flip operation together ( $iY$ ) gate, the state will become

$$(iY \otimes I)|\psi\rangle = |01\rangle - |10\rangle.$$

Bob deduces which Bell basis state the qubits are in by operating on the pair with the *CNOT* operation (i.e *XOR* gate) and measuring the target bit and thus distinguishing  $|00\rangle \pm |11\rangle$  from  $|01\rangle \pm |10\rangle$ . He then operates the H-gate on the remaining qubit and measures it to find the sign in the superposition (see Fig.(4.1)).

Dense coding is difficult to implement and so has no practical value as a standard communication method. However, it can permit secure communication: the qubit sent by someone will only yield the two classical information bits to some other in

possession of the entangled partner qubit. A laboratory demonstration of the main features is described by Mattle et al (1996) [10], Weinfurter (1994) and Braunstein and Mann (1995) discussed some of the methods employed, based on a source of EPR photon pairs from parametric down-conversion. In the next section we are going to model theoretically the experimental setup of dense coding realistically, described in Mattle et al. (1996) [10].

### 4.3 Theoretical Model of Quantum Dense Coding

Quantum mechanics also provides an opportunity to encode information in superposition of the classical combinations, an appropriate basis is formed by maximally entangled Bell states

$$\begin{aligned}
 |\psi^+\rangle &= (|H\rangle|V\rangle + |V\rangle|H\rangle)/\sqrt{2}, \\
 |\psi^-\rangle &= (|H\rangle|V\rangle - |V\rangle|H\rangle)/\sqrt{2}, \\
 |\phi^+\rangle &= (|H\rangle|H\rangle + |V\rangle|V\rangle)/\sqrt{2}, \\
 |\phi^-\rangle &= (|H\rangle|H\rangle - |V\rangle|V\rangle)/\sqrt{2}.
 \end{aligned}
 \tag{4.3.1}$$

These orthogonal states still span the four dimensional Hilbert space, implying that using the two particles we again can encode 2 bits of information, but now by just manipulating just one of the two particles. This is achieved in the quantum dense coding for transmitting 2 bits of information per two states. Let us say, initially, Alice and Bob each gets one particle of an entangled pair in state  $|\psi^+\rangle$ . To encode information Bob performs any of the four unitary operations on a particle in his possession. As in the case of entanglement swapping Mattle et al. considered the polarization entangled pairs because of higher stability and more reliable methods for manipulating polarized beams, as opposed to momentum entangled photons [3]. Thus, to encode information on polarization entangled photons such transformations are (i) identity operation; (ii) polarization flip operation i.e ( $|V\rangle \rightarrow |H\rangle$ ) and ( $|H\rangle \rightarrow |V\rangle$ ); (iii) polarization dependent phase shift (iv) rotation and phase shift together. Hence these four manipulations results in the four Bell states, four distinguishable messages i.e 2 bits of information can be sent via Bob's encoded particle of two

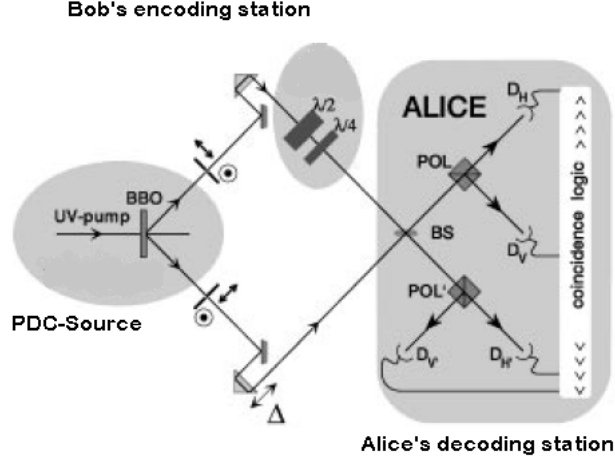


Figure 4.2: Experimental model for quantum dense coding [10]. To detect  $|\psi^+\rangle$ , both retardation plates are set to vertical orientation so there will be no change in beam coming from Bob's encoding station.

particle system to Alice, who can read this information by determining the Bell state of two-particle system.

The realistic model of quantum dense coding experiment which is going to be given here based on the experiment done by Mattle et al. in [10]. The polarization entangled photons are generated by nonlinear type-II down-conversion and sent to Bob who encode the information on them by some unitary transformation; then Alice does some measurement to decode them. Following this order we have calculated the state generated by a type-II PDC source used for quantum dense coding in Eq.(2.5.21), given as

$$|\chi\rangle = \exp[2\omega(\chi)] \exp[\phi(\chi)(\hat{a}_h^\dagger \hat{b}_v^\dagger - \hat{a}_v^\dagger \hat{b}_h^\dagger)] |vac\rangle. \quad (4.3.2)$$

As shown in the Fig.(4.2) after emitting from the source, one beam is directed towards Bob's encoding station and the other one is sent directly to Alice's Bell state analyzer. The two beams are made to overlap to equalize the path lengths to well within the coherence length of down converted photons ( $l_c = 100\mu m$ ), in order to observe interference of two photons at the beam splitter. Bob wants to communicate with Alice so he encodes the information on that beam using half wave plate for changing the polarization and quarter wave plate for changing the polarization phase shift <sup>1</sup>. The beam manipulated in this way is then combined

<sup>1</sup>The component polarized along the axis of the quarterwave plate is advanced only by  $\frac{\pi}{2}$  relative to the other. Reorienting the optical axis from vertical to horizontal causes a net phase change of  $\pi$  between  $|H\rangle$  and  $|V\rangle$ .

with the other beam at Alice's Bell state analyzer which consisted of a beam splitter followed by two polarization beam splitters (channel polarizers) at the two output ports of beam splitter and then these beams are detected at four detectors to get coincidence analysis.

Let us consider first the output state as  $\psi^-$ . To get interference we introduced a phase shifter operator  $\exp(-i\theta\hat{N})$ , where the angle  $\theta = \Delta / \lambda$  represents the relative phase shift between two paths,  $\Delta$  is the path length detuning measured in micrometers [23] and  $\hat{N}$  simply understood as the number operator. The two beams are made to overlap to equalize the path lengths to well within the coherence length of down converted photons ( $l_c = 100\mu m$ ), in order to observe interference of two photons at the beam splitter. The action of the beam splitter is given as

$$\hat{U}_B = \frac{1}{\sqrt{2}} \begin{pmatrix} 1 & 1 \\ -1 & 1 \end{pmatrix}. \quad (4.3.3)$$

After applying the beam splitter transformation

$$\begin{pmatrix} a_h \\ b_h \end{pmatrix} \xrightarrow{\hat{U}_B^\dagger} \begin{pmatrix} a'_h \\ b'_h \end{pmatrix}$$

, and

$$\begin{pmatrix} a_v \\ b_v \end{pmatrix} \xrightarrow{\hat{U}_B^T} \begin{pmatrix} a'_v \\ b'_v \end{pmatrix}.$$

For the beam splitter being used here

$$\hat{U}_B^\dagger = \hat{U}_B^T = \frac{1}{\sqrt{2}} \begin{pmatrix} 1 & 1 \\ -1 & 1 \end{pmatrix}, \quad (4.3.4)$$

while the number operator here will be

$$\hat{N} = \hat{a}_h^\dagger \hat{a}_h + \hat{a}_v^\dagger \hat{a}_v, \quad (4.3.5)$$

as is clear from the number operator form above, Bob is encoding information only on the qubit in his possession. Now we apply the phase shifter operator  $\exp(-i\frac{\Delta}{\lambda}N)$ ,



and the beam splitter on the state given in Eq.(4.3.2), we get

$$\begin{aligned} \hat{U}_B \exp\left(\frac{-iN \Delta}{\lambda}\right)|\chi\rangle &= \hat{U}_B \exp\left[\left(\frac{-i \Delta}{\lambda}\right)(\hat{a}_h^\dagger \hat{a}_h + \hat{a}_v^\dagger \hat{a}_v)\right] \\ &\quad \exp[2\omega(\chi)] \exp[\phi(\chi)(\hat{a}_h^\dagger \hat{b}_v^\dagger - \hat{a}_v^\dagger \hat{b}_h^\dagger)] \times |vac\rangle \end{aligned} \quad (4.3.6)$$

$$\begin{aligned} &= \exp[2\omega(\chi)] \exp\left[\left(\frac{-i \Delta}{\lambda}\right)\left\{\frac{(\hat{a}_h^\dagger - \hat{b}_h^\dagger)(\hat{a}_h - \hat{b}_h)}{2} + \frac{(\hat{a}_v^\dagger - \hat{b}_v^\dagger)(\hat{a}_v - \hat{b}_v)}{2}\right\}\right] \times \\ &\quad \exp\left[\phi\left\{\frac{(\hat{a}_h^\dagger - \hat{b}_h^\dagger)(\hat{a}_v^\dagger + \hat{b}_v^\dagger)}{2} - \frac{(\hat{a}_v^\dagger - \hat{b}_v^\dagger)(\hat{a}_h^\dagger + \hat{b}_h^\dagger)}{2}\right\}\right] \times |vac\rangle \end{aligned} \quad (4.3.7)$$

,

$$\begin{aligned} \hat{U}_B \exp\left(\frac{-iN \Delta}{\lambda}\right)|\chi\rangle &= \exp\left[\left(\frac{-i \Delta}{\lambda}\right)\left(\frac{\hat{a}_h^\dagger \hat{a}_h - \hat{a}_h^\dagger \hat{b}_h - \hat{b}_h^\dagger \hat{a}_h + \hat{b}_h^\dagger \hat{b}_h}{2} + \frac{\hat{a}_v^\dagger \hat{a}_v - \hat{a}_v^\dagger \hat{b}_v - \hat{b}_v^\dagger \hat{a}_v + \hat{b}_v^\dagger \hat{b}_v}{2}\right)\right] \\ &\quad \times \exp\left[\phi\left(\frac{\hat{a}_h^\dagger \hat{a}_v^\dagger + \hat{a}_h^\dagger \hat{b}_v^\dagger - \hat{b}_h^\dagger \hat{a}_v^\dagger - \hat{b}_h^\dagger \hat{b}_v^\dagger}{2} - \frac{\hat{a}_v^\dagger \hat{a}_h^\dagger + \hat{a}_v^\dagger \hat{b}_h^\dagger - \hat{b}_v^\dagger \hat{a}_h^\dagger - \hat{b}_v^\dagger \hat{b}_h^\dagger}{2}\right)\right] \\ &\quad \times \exp[2\omega(\chi)]|vac\rangle. \end{aligned} \quad (4.3.8)$$

To decompose these exponential terms, it is convenient to use the Baker-Campbell-Hausdorff formula

$$\exp(X + Y) := \exp(X) \exp(Y) \exp\left(-\frac{1}{2}[X, Y]\right). \quad (4.3.9)$$

As we know, this formula holds under the condition that  $[X, Y] = 0$  and  $[X, [X, Y]] = 0$ , so considering the first exponential term in Eq.(4.3.8) only we get

$$\begin{aligned} &\exp\left[\left(\frac{-i \Delta}{\lambda}\right)\left(\frac{\hat{a}_h^\dagger \hat{a}_h - \hat{a}_h^\dagger \hat{b}_h - \hat{b}_h^\dagger \hat{a}_h + \hat{b}_h^\dagger \hat{b}_h}{2} + \frac{\hat{a}_v^\dagger \hat{a}_v - \hat{a}_v^\dagger \hat{b}_v - \hat{b}_v^\dagger \hat{a}_v + \hat{b}_v^\dagger \hat{b}_v}{2}\right)\right] \\ &= \exp\left[\left(\frac{-i \Delta}{\lambda}\right)(\hat{a}_h^\dagger \hat{a}_h)\right] \exp\left[\left(\frac{-i \Delta}{\lambda}\right)(\hat{b}_h^\dagger \hat{b}_h)\right] \times \exp\left[\left(\frac{i \Delta}{\lambda}\right)(\hat{a}_h^\dagger \hat{b}_h + \hat{b}_h^\dagger \hat{a}_h)\right] \\ &\quad \times \exp\left[\left(\frac{-i \Delta}{\lambda}\right)(\hat{a}_v^\dagger \hat{a}_v)\right] \exp\left[\left(\frac{-i \Delta}{\lambda}\right)(\hat{b}_v^\dagger \hat{b}_v)\right] \exp\left[\left(\frac{i \Delta}{\lambda}\right)(\hat{a}_v^\dagger \hat{b}_v + \hat{b}_v^\dagger \hat{a}_v)\right]. \end{aligned} \quad (4.3.10)$$

The 3rd exponential term in Eq.(4.3.10) cannot be decomposed using BCH formula given in Eq.(4.3.9) as this does not satisfy the conditions required to hold that formula. So for this we will use generalized Baker-Campbell-Hausdorff formula. Let us define

$$\hat{A}_+ := \hat{a}_h^\dagger \hat{b}_h, \quad \hat{A}_- := \hat{b}_h^\dagger \hat{a}_h, \quad \hat{A}_z := \frac{1}{2}(\hat{b}_h^\dagger \hat{b}_h - \hat{a}_h^\dagger \hat{a}_h). \quad (4.3.11)$$

These operators form a bosonic representation of the SU(2) Lie algebra, as they obey the commutation relations of the generators of the latter. The following decomposi-

tion formula holds for the exponential factors of SU(2) according to [3]:

$$\exp i\tilde{\alpha}[\theta_+ A_+ + \theta_z A_z + \theta_- A_-] = \exp [g_+(\tilde{\alpha})A_+] \exp [g_z(\tilde{\alpha})A_z] \exp [g_-(\tilde{\alpha})A_-], \quad (4.3.12)$$

where the functions  $g_{\pm}(\tilde{\alpha}), g_z(\tilde{\alpha})$  are defined as

$$g_{\pm}(\tilde{\alpha}) := \frac{i\theta_{\pm}}{\Gamma} \frac{\sin(\Gamma_1 \tilde{\alpha})}{\Gamma \cos(\Gamma \tilde{\alpha}) - i\theta_z \sin(\Gamma \tilde{\alpha})/2\Gamma}, \quad (4.3.13)$$

$$g_z(\tilde{\alpha}) := -2 \ln[\cos(\Gamma \tilde{\alpha}) - i\frac{\theta_z}{2\Gamma} \sin(\Gamma \tilde{\alpha})], \quad (4.3.14)$$

with

$$\Gamma := \theta_+ \theta_- + \frac{\theta_z^2}{4}. \quad (4.3.15)$$

Thus using generalized BCH decomposition relation the Eq.(4.3.10) becomes

$$\begin{aligned} & \exp \left[ \left( \frac{-i \Delta}{2\lambda} \right) \left( \frac{\hat{a}_h^\dagger \hat{a}_h - \hat{a}_h^\dagger \hat{b}_h - \hat{b}_h^\dagger \hat{a}_h + \hat{b}_h^\dagger \hat{b}_h}{2} + \frac{\hat{a}_v^\dagger \hat{a}_v - \hat{a}_v^\dagger \hat{b}_v - \hat{b}_v^\dagger \hat{a}_v + \hat{b}_v^\dagger \hat{b}_v}{2} \right) \right] \\ = & \exp \left[ \left( \frac{-i \Delta}{2\lambda} \right) \hat{a}_h^\dagger \hat{a}_h \right] \exp \left[ \left( \frac{-i \Delta}{2\lambda} \right) \hat{b}_h^\dagger \hat{b}_h \right] \exp \left[ i \tan \left( \frac{\Delta}{2\lambda} \right) \hat{a}_h^\dagger \hat{b}_h \right] \\ & \times \exp \left[ -\ln \cos \left( \frac{\Delta}{2\lambda} \right) \hat{b}_h^\dagger \hat{b}_h \right] \exp \left[ \ln \cos \left( \frac{\Delta}{2\lambda} \right) \hat{a}_h^\dagger \hat{a}_h \right] \exp \left[ i \tan \left( \frac{\Delta}{2\lambda} \right) \hat{b}_h^\dagger \hat{a}_h \right] \\ & \times \exp \left[ \left( \frac{-i \Delta}{2\lambda} \right) \hat{a}_v^\dagger \hat{a}_v \right] \exp \left[ \left( \frac{-i \Delta}{2\lambda} \right) \hat{b}_v^\dagger \hat{b}_v \right] \exp \left[ i \tan \left( \frac{\Delta}{2\lambda} \right) \hat{a}_v^\dagger \hat{b}_v \right] \\ & \times \exp \left[ -\ln \cos \left( \frac{\Delta}{2\lambda} \right) \hat{b}_v^\dagger \hat{b}_v \right] \exp \left[ \ln \cos \left( \frac{\Delta}{2\lambda} \right) \hat{a}_v^\dagger \hat{a}_v \right] \exp \left[ i \tan \left( \frac{\Delta}{2\lambda} \right) \hat{b}_v^\dagger \hat{a}_v \right]. \end{aligned} \quad (4.3.16)$$

The 2nd exponential factor in Eq.(4.3.8) is much easier to decompose as the operators of both modes  $(\hat{a}_h^\dagger, \hat{a}_h, \hat{a}_v^\dagger, \hat{a}_v)$  commute with each other. So that term will reduce as

$$\begin{aligned} & \exp \left[ \phi \left( \frac{\hat{a}_h^\dagger \hat{a}_v^\dagger + \hat{a}_h^\dagger \hat{b}_v^\dagger - \hat{b}_h^\dagger \hat{a}_v^\dagger - \hat{b}_h^\dagger \hat{b}_v^\dagger}{2} - \frac{\hat{a}_v^\dagger \hat{a}_h^\dagger + \hat{a}_v^\dagger \hat{b}_h^\dagger - \hat{b}_v^\dagger \hat{a}_h^\dagger - \hat{b}_v^\dagger \hat{b}_h^\dagger}{2} \right) \right] \\ = & \exp [\phi(\hat{a}_h^\dagger \hat{b}_v^\dagger)] \exp [-\phi(\hat{a}_v^\dagger \hat{b}_h^\dagger)]. \end{aligned} \quad (4.3.17)$$

Hence Eq.(4.3.8) can be written as

$$\begin{aligned} \hat{U}_B \exp \left( \frac{-iN \Delta}{\lambda} \right) |\chi\rangle & = \exp [2\omega(\chi)] \exp \left[ \left( \frac{-i \Delta}{2\lambda} \right) \hat{a}_h^\dagger \hat{a}_h \right] \exp \left[ \left( \frac{-i \Delta}{2\lambda} \right) \hat{b}_h^\dagger \hat{b}_h \right] \exp \left[ i \tan \left( \frac{\Delta}{2\lambda} \right) \hat{a}_h^\dagger \hat{b}_h \right] \\ & \times \exp \left[ -\ln \cos \left( \frac{\Delta}{2\lambda} \right) \hat{b}_h^\dagger \hat{b}_h \right] \exp \left[ \ln \cos \left( \frac{\Delta}{2\lambda} \right) \hat{a}_h^\dagger \hat{a}_h \right] \exp \left[ i \tan \left( \frac{\Delta}{2\lambda} \right) \hat{b}_h^\dagger \hat{a}_h \right] \\ & \times \exp \left[ \left( \frac{-i \Delta}{2\lambda} \right) \hat{a}_v^\dagger \hat{a}_v \right] \exp \left[ \left( \frac{-i \Delta}{2\lambda} \right) \hat{b}_v^\dagger \hat{b}_v \right] \exp \left[ i \tan \left( \frac{\Delta}{2\lambda} \right) \hat{a}_v^\dagger \hat{b}_v \right] \\ & \times \exp \left[ -\ln \cos \left( \frac{\Delta}{2\lambda} \right) \hat{b}_v^\dagger \hat{b}_v \right] \exp \left[ \ln \cos \left( \frac{\Delta}{2\lambda} \right) \hat{a}_v^\dagger \hat{a}_v \right] \exp \left[ i \tan \left( \frac{\Delta}{2\lambda} \right) \hat{b}_v^\dagger \hat{a}_v \right] \\ & \times \exp [\phi(\hat{a}_h^\dagger \hat{b}_v^\dagger)] \exp [-\phi(\hat{a}_v^\dagger \hat{b}_h^\dagger)] |vac\rangle, \end{aligned} \quad (4.3.18)$$

$$\begin{aligned}
\hat{U}_B \exp\left(\frac{-iN \Delta}{\lambda}\right)|\chi\rangle &= \exp[2\omega(\chi)] \exp\left[\left(\frac{-i \Delta}{2\lambda}\right)\hat{a}_h^\dagger \hat{a}_h\right] \exp\left[\left(\frac{-i \Delta}{2\lambda}\right)\hat{b}_h^\dagger \hat{b}_h\right] \sum_{i=0}^{\infty} \frac{1}{i!} [i \tan\left(\frac{\Delta}{2\lambda}\right)\hat{a}_h^\dagger \hat{b}_h]^i \\
&\times \exp\left[-\ln \cos\left(\frac{\Delta}{2\lambda}\right)\hat{b}_h^\dagger \hat{b}_h\right] \exp\left[\ln \cos\left(\frac{\Delta}{2\lambda}\right)\hat{a}_h^\dagger \hat{a}_h\right] \sum_{j=0}^{\infty} \frac{1}{j!} [i \tan\left(\frac{\Delta}{2\lambda}\right)\hat{b}_h^\dagger \hat{a}_h]^j \\
&\times \exp\left[\left(\frac{-i \Delta}{2\lambda}\right)\hat{a}_v^\dagger \hat{a}_v\right] \exp\left[\left(\frac{-i \Delta}{2\lambda}\right)\hat{b}_v^\dagger \hat{b}_v\right] \sum_{k=0}^{\infty} \frac{1}{k!} [i \tan\left(\frac{\Delta}{2\lambda}\right)\hat{a}_v^\dagger \hat{b}_v]^k \\
&\times \exp\left[-\ln \cos\left(\frac{\Delta}{2\lambda}\right)\hat{b}_v^\dagger \hat{b}_v\right] \exp\left[\ln \cos\left(\frac{\Delta}{2\lambda}\right)\hat{a}_v^\dagger \hat{a}_v\right] \sum_{l=0}^{\infty} \frac{1}{l!} [i \tan\left(\frac{\Delta}{2\lambda}\right)\hat{b}_v^\dagger \hat{a}_v]^l \\
&\times \sum_{m=0}^{\infty} \frac{\phi^m}{m!} (\hat{a}_h^\dagger \hat{b}_v^\dagger)^m \sum_{n=0}^{\infty} \frac{-\phi^n}{n!} (\hat{a}_v^\dagger \hat{b}_h^\dagger)^n |vac\rangle, \tag{4.3.19}
\end{aligned}$$

$$\begin{aligned}
\hat{U}_B \exp\left(\frac{-iN \Delta}{\lambda}\right)|\chi\rangle &= \exp[2\omega(\chi)] \sum_{n=0}^{\infty} \sum_{m=0}^{\infty} \sum_{l=0}^{\infty} \sum_{k=0}^{\infty} \sum_{j=0}^{\infty} \sum_{i=0}^{\infty} \phi^{m+n} (-1)^n [i \tan\left(\frac{\Delta}{2\lambda}\right)]^{i+j+k+l} \\
&\times \exp\left[\left(\frac{-i \Delta}{2\lambda}\right)(m-j+i)\right] \exp\left[\left(\frac{-i \Delta}{2\lambda}\right)(n+j-i)\right] \\
&\times \exp\left[-\ln \cos\left(\frac{\Delta}{2\lambda}\right)(n+j)\right] \exp\left[\ln \cos\left(\frac{\Delta}{2\lambda}\right)(m-j)\right] \\
&\times \exp\left[\left(\frac{-i \Delta}{2\lambda}\right)(n-l+k)\right] \exp\left[\left(\frac{-i \Delta}{2\lambda}\right)(m+l-k)\right] \\
&\times \exp\left[-\ln \cos\left(\frac{\Delta}{2\lambda}\right)(m+l)\right] \exp\left[\ln \cos\left(\frac{\Delta}{2\lambda}\right)(n-l)\right] \\
&\times \frac{m!n!(m+l)!(n+j)!}{m!n!l!k!j!i!(n-l)!(m-j)!} \frac{\sqrt{(n-l+k)!(m-j+i)!}}{\sqrt{(m+l-k)!(n+j-i)!}} \\
&\times |m-j+i, n-l+k, m+l-k, n+j-i\rangle, \tag{4.3.20}
\end{aligned}$$

$$\begin{aligned}
\hat{U}_B \exp\left(\frac{-iN \Delta}{\lambda}\right)|\chi\rangle &= \exp[2\omega(\chi)] \sum_{n=0}^{\infty} \sum_{m=0}^{\infty} \sum_{l=0}^{\infty} \sum_{k=0}^{\infty} \sum_{j=0}^{\infty} \sum_{i=0}^{\infty} \phi^{m+n} (-1)^n [i \tan\left(\frac{\Delta}{2\lambda}\right)]^{i+j+k+l} \\
&\times \exp\left[\left(\frac{-i \Delta}{2\lambda}\right)(m+n)\right] \exp\left[-\ln \cos\left(\frac{\Delta}{2\lambda}\right)(-2j-2l)\right] \\
&\times \frac{(m+l)!(n+j)!}{l!k!j!i!(n-l)!(m-j)!} \frac{\sqrt{(n-l+k)!(m-j+i)!}}{\sqrt{(m+l-k)!(n+j-i)!}} \\
&\times |m-j+i, n-l+k, m+l-k, n+j-i\rangle. \tag{4.3.21}
\end{aligned}$$

To find the state which will come out after passing through the beam splitter we apply projection operator on the above state in the following form,

$$\prod_{a'_h, a'_v, b'_v, b'_h}^{(i'j'k'l')} := (|i'\rangle\langle i'|)_{a'_h} \otimes (|j'\rangle\langle j'|)_{a'_v} \otimes (|k'\rangle\langle k'|)_{b'_v} \otimes (|l'\rangle\langle l'|)_{b'_h}. \tag{4.3.22}$$

The modes  $a_h, a_v, b_v, b_h$  are the output modes of the beam splitter. The operator  $\hat{U}_B$  represents the unitary evolution corresponding to the beam splitter transformation. Here and in what follows,  $|n\rangle$  denotes an n-photon Fock state and it should be clear from the context to which mode it refers. Accordingly,  $(|i'\rangle\langle i'|)_{a'_h}$  represents a

projection operator corresponding to the Fock state  $|i\rangle$  of the mode  $a'_h$  and so on.

Thus

$$\begin{aligned}
\prod_{a'_h, a'_v, b'_v, b'_h}^{(i'j'k'l')} \hat{U}_B \exp\left(\frac{-iN\Delta}{\lambda}\right) |\chi\rangle &= \exp[2\omega(\chi)] \sum_{n=0}^{\infty} \sum_{m=0}^{\infty} \sum_{l=0}^{\infty} \sum_{k=0}^{\infty} \sum_{j=0}^{\infty} \sum_{i=0}^{\infty} \phi^{m+n} (-1)^n \\
&\quad [i \tan(\frac{\Delta}{2\lambda})]^{i+j+k+l} \times \exp\left[\left(\frac{-i\Delta}{2\lambda}\right)(m+n)\right] \\
&\quad \exp\left[-\ln \cos\left(\frac{\Delta}{2\lambda}\right)(-2j-2l)\right] \\
&\quad \times \frac{(m+l)!(n+j)!}{l!k!j!i!(n-l)!(m-j)!} \frac{\sqrt{(n-l+k)!(m-j+i)!}}{\sqrt{(m+l-k)!(n+j-i)!}} \\
&\quad \times \delta_{i', m-j+i} \delta_{j', n-l+k} \delta_{k', m+l-k} \delta_{l', n+j-i} |i'j'k'l'\rangle, \quad (4.3.23)
\end{aligned}$$

$$\begin{aligned}
\prod_{a'_h, a'_v, b'_v, b'_h}^{(i'j'k'l')} \hat{U}_B \exp\left(\frac{-iN\Delta}{\lambda}\right) |\chi\rangle &= \exp[2\omega(\chi)] \sum_{n=0}^{\infty} \sum_{m=0}^{\infty} \sum_{l=0}^{\infty} \sum_{j=0}^{\infty} \phi^{m+n} (-1)^n \\
&\quad [i \tan(\frac{\Delta}{2\lambda})]^{i'+2j+2l-k'} \times \exp\left[\left(\frac{-i\Delta}{2\lambda}\right)(m+n)\right] \\
&\quad \exp\left[-\ln \cos\left(\frac{\Delta}{2\lambda}\right)(-2j-2l)\right] \\
&\quad \frac{(m+l)!(n+j)!}{l!j!(m+l-k')!(i'-m+j)!(n-l)!(m-j)!} \\
&\quad \times \frac{\sqrt{j'!i'!}}{\sqrt{k'!l'!}} \delta_{i'-m, n-l'} \delta_{j'-n, m-k'} |i'j'k'l'\rangle, \quad (4.3.24)
\end{aligned}$$

$$\begin{aligned}
\prod_{a'_h, a'_v, b'_v, b'_h}^{(i'j'k'l')} \hat{U}_B \exp\left(\frac{-iN\Delta}{\lambda}\right) |\chi\rangle &= \exp[2\omega(\chi)] \sum_{m=0}^{\infty} \sum_{l=0}^n \sum_{j=0}^m \phi^{m+n} (-1)^{i'-m+l} \\
&\quad [i \tan(\frac{\Delta}{2\lambda})]^{i'-k'+2(j+l)} \times \exp\left[\left(\frac{-i\Delta}{2\lambda}\right)(m+n)\right] \\
&\quad \exp\left[-\ln \cos\left(\frac{\Delta}{2\lambda}\right)(-2j-2l)\right] \\
&\quad \times \frac{(m+l)!(j'-k'-m+j)!}{l!j!(m-j)!(m+l-k')!(i'-m+j)!(i'+l'-m-l)!} \\
&\quad \times \sqrt{\frac{i'!j'!}{k'!l'!}} \delta_{i'-m, n-l'} \delta_{j'-n, m-k'} |i'j'k'l'\rangle, \quad (4.3.25)
\end{aligned}$$

$$\begin{aligned}
\prod_{a'_h, a'_v, b'_v, b'_h}^{(i'j'k'l')} \hat{U}_B \exp\left(\frac{-iN\Delta}{\lambda}\right) |\chi\rangle &= \exp[2\omega(\chi)] \sum_{m=0}^{\infty} \sum_{l=0}^{j'+k'-m} \sum_{j=0}^m \phi^{i'+l'} (-1)^{i'-m+l'} \\
& [i \tan\left(\frac{\Delta}{2\lambda}\right)]^{i'-k'+2(j+l)} \times \exp\left[\left(\frac{-i\Delta}{2\lambda}\right)(i'+l')\right] \\
& \exp\left[-\ln \cos\left(\frac{\Delta}{2\lambda}\right)(-2j-2l)\right] \\
& \times \frac{(m+l)!(j'-k'-m+j)!}{l!j!(m-j)!(m+l-k')!(i'-m+j)!(i'+l'-m-l)!} \\
& \times \sqrt{\frac{i'!j'!}{k'!l'!}} \delta_{i'+l', j'+k'} |i'j'k'l'\rangle, \tag{4.3.26}
\end{aligned}$$

$l$  will remain positive only for  $m \leq j' + k'$ . So by changing the summation over  $m$ , we get

$$\begin{aligned}
\prod_{a'_h, a'_v, b'_v, b'_h}^{(i'j'k'l')} \hat{U}_B \exp\left(\frac{-iN\Delta}{\lambda}\right) |\chi\rangle &= \exp[2\omega(\chi)] \sum_{m=0}^{j'+k'} \sum_{l=0}^{j'+k'-m} \sum_{j=0}^m \phi^{i'+l'} (-1)^{i'-m+l'} \\
& [i \tan\left(\frac{\Delta}{2\lambda}\right)]^{i'-k'+2(j+l)} \times \exp\left[\left(\frac{-i\Delta}{2\lambda}\right)(i'+l')\right] \\
& \exp\left[-\ln \cos\left(\frac{\Delta}{2\lambda}\right)(-2j-2l)\right] \\
& \times \frac{(m+l)!(j'-k'-m+j)!}{l!j!(m-j)!(m+l-k')!(i'-m+j)!(i'+l'-m-l)!} \\
& \times \sqrt{\frac{i'!j'!}{k'!l'!}} \delta_{i'+l', j'+k'} |i'j'k'l'\rangle. \tag{4.3.27}
\end{aligned}$$

Now if  $i' - m + j > 0 \implies j > m - i'$

$$m - j > 0 \implies j < m$$

$$i' + l' - m - l > 0 \implies l < i' + l' - m$$

$$m + l - k' > 0 \implies l > k' - m$$

$$\begin{aligned}
\prod_{a'_h, a'_v, b'_v, b'_h}^{(i'j'k'l')} \hat{U}_B \exp\left(\frac{-iN\Delta}{\lambda}\right) |\chi\rangle &= \exp[2\omega(\chi)] \sum_{m=0}^{i'+l'} \sum_{l=\max\{0, k'-m\}}^{i'+l'-m} \sum_{j=\max\{0, m-i'\}}^m \phi^{i'+l'} (-1)^{i'-m+l'} \\
& \times [i \tan\left(\frac{\Delta}{2\lambda}\right)]^{i'-k'+2(j+l)} \exp\left[\left(\frac{-i\Delta}{2\lambda}\right)(i'+l')\right] \\
& \times \exp\left[-\ln \cos\left(\frac{\Delta}{2\lambda}\right)(-2j-2l)\right] \\
& \times \frac{(m+l)!(j'-k'-m+j)!}{l!j!(m-j)!(m+l-k')!(i'-m+j)!(i'+l'-m-l)!} \\
& \times \sqrt{\frac{i'!j'!}{k'!l'!}} \delta_{i'+l', j'+k'} |i'j'k'l'\rangle. \tag{4.3.28}
\end{aligned}$$

Thus the probability for quantum dense coding experiment in case of ideal detection will be

$$P(i'j'k'l') = \left\| \prod_{a'_h, a'_v, b'_v, b'_h}^{(i'j'k'l')} \hat{U}_B \exp\left(\frac{-iN \Delta}{\lambda}\right) |\chi\rangle \right\|^2. \quad (4.3.29)$$

We have calculated the probabilities for photon number discriminating detectors and ideal threshold detectors, both for the ideal case and in the presence of dark counts. As mentioned earlier, given an actual readout  $(qrst)$  of an imperfect Bell measurement with inaccurate detectors including dark counts, we infer what an ideal four tuple of detectors would have yielded i.e read out  $(ijkl)$  with probability  $P_{ijkl}^{qrst} := P(ijkl|qrst)$  using Bayesian inference approach,

$$P_{ijkl}^{qrst} \equiv P(ijkl|qrst) = \frac{P(qrst|ijkl)P(ijkl)}{P(qrst)}. \quad (4.3.30)$$

$P(ijkl)$  is the probability of hypothetical ideal measurement readout  $(ijkl)$  which in our case of dense coding is given in Eq.(4.3.29). In an actual experiment, however, detectors have efficiency less than 100% and in addition exhibit dark counts. Hence we can calculate the conditional probability  $P(qrst|ijkl)$  for all the possible events  $(ijkl)$ . As the four detectors are statistically independent from one another, these probabilities can be factorized into four terms,

$$P_{\eta, \rho_{dc}}(qrst|ijkl) = P_{\eta, \rho_{dc}}(q|i)P_{\eta, \rho_{dc}}(r|j) \times P_{\eta, \rho_{dc}}(s|k)P_{\eta, \rho_{dc}}(t|l) \quad (4.3.31)$$

Each of these probabilities has been calculated earlier. By combining the above equation with Eq.(4.3.29), we can calculate the posterior probability of ideal hypothetical readout  $(ijkl)$  given the evidence  $(qrst)$  has happened.

$$P_{ijkl}^{qrst}(\chi, \eta, \rho_{dc}) = P_{\eta, \rho_{dc}}(q|i)P_{\eta, \rho_{dc}}(r|j) \times P_{\eta, \rho_{dc}}(s|k)P_{\eta, \rho_{dc}}(t|l) \times P(i'j'k'l'). \quad (4.3.32)$$

We have found the hypothetical probability of the state  $|\psi^-\rangle$  in case of perfect detectors given in Eq.(4.3.29) for quantum dense coding experiment. To detect the other three Bell state we will have to include the half wave plate and quarter wave plate and by changing their orientations we can detect two out of remaining three Bell states. In principle, all four Bell states should detect at the detectors but yet it is impossible to distinguish between  $|\phi^+\rangle$  and  $|\phi^-\rangle$ . The two photons in this case are

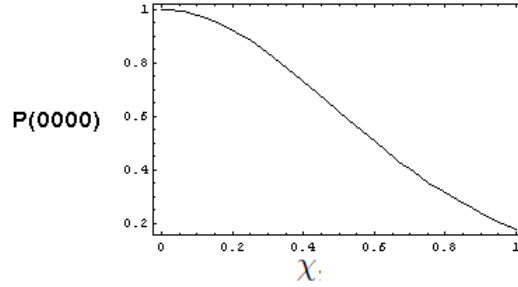


Figure 4.3: Curve shows that for the given value of  $\chi$  the probability  $P(0000)$  along y-axis is maximum and it will start decreasing when no. of photons striking at the detectors increases with the passage of time.

detected at either of the detectors  $D_h$ ,  $D_v$ ,  $D'_h$  and  $D'_v$  thus we cannot distinguish between the two correlated photons. We draw the above calculated hypothetical probability with different values of nonlinearity of the down converted crystal. In this present setting of our model to detect  $|\psi^-\rangle$  state, the other Bell states could not then be generated with respective setting. For numerical simulations we choose the value of  $\chi = 1$  to calculate the probability of  $|\psi^-\rangle$  state. The dark counts effect becomes stronger as the number of photon incident at the detectors increases, so the probability  $P(i'j'k'l')$  decreases. So our result of hypothetical probability by

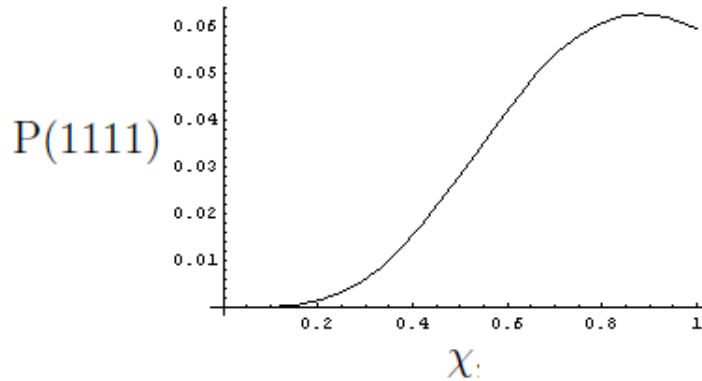


Figure 4.4: Curve shows that for the given value of  $\chi$  the probability  $P(1111)$  is less than  $P(0000)$  at  $\chi = 1$  as the no. of photons striking at the detectors increases.

considering the detectors ideal is similar as given by Mattle et al. in [10]. The large value of  $\chi$  also result in increase of dark counts so usually we take smaller values of  $\chi$  to reduce the effect of dark counts.

# Chapter 5

## Conclusion

### 5.1 Sources and Detectors

In this dissertation non-ideal sources and detectors have been considered. Ideal photon pair sources would create exactly one entangled photon pair on demand. Such sources do not exist yet; realistic sources are probabilistic in nature. The rate of pair generation using PDC crystal is proportional to nonlinearity  $\chi^2$ , the strength of the classical pump field and interaction time. The role of the vacuum state in equation below which is in chapter 2 in Eq.(2.5.4).

$$Y(\gamma) |vac\rangle = |vac\rangle + \frac{i\gamma}{2} |0110\rangle, \quad (5.1.1)$$

is to allow for the particular feature that the generation of the desired photon pair occurs at random instances of time. More precisely, when a pump pulse is sent, it will either lead to the down conversion or not. The strong vacuum component shows that there is a high probability that PDC will not take place at all.

The randomness of photon pair generation can be decreased by using a PDC crystal with large value of nonlinearity  $\chi^2$  or stronger pump fields, but this costs the increased probability of emission of multipairs of photons, which really affects the experiment and should be avoided as far as possible. However, multi-pair emission effect cannot be excluded completely. Too small a value of  $\chi$  leads to a strong vacuum contribution, thus most of the time sources do not emit any photon pair. While much higher values of  $\chi$  also result in decrease of entanglement in the final



quantum state after entanglement swapping and as such have an adverse impact.

The realistic models of the detectors used for these processes have also been discussed here. We have made a distinction between photon-number discriminating detectors and threshold detectors. In practice, however, detectors cannot measure the photon's number efficiently but instead effectively measure if there are no photons in a mode or atleast one photon. Such detectors are referred as threshold detectors and for this reason these are considered more realistic than photon number discriminating detectors. We calculated the probabilities for both type of detectors realistically and in the presence of dark counts.

## 5.2 Theoretical Entanglement Swapping

These realistic models of entanglement swapping and quantum dense coding could be very helpful to understand these processes at the physical level. We have derived the actual quantum state of the remaining modes  $a$  and  $d$  depending on the result of a noisy Bell measurement with probabilistic sources and imperfect detectors for entanglement swapping experiment. The most important advantage of this model is to provide this quantum state for any given photon-pair production rate  $\chi$ , any given efficiency  $\eta$  of the detectors and any reasonable dark counts probability  $\rho_{dc}$ . One can make predictions with regard to any quantity of interest using this calculated quantum state, specifically, one can calculate the entanglement of the remaining modes. It has been shown that predictions of our theory are in close accordance with experimental entanglement swapping.

## 5.3 Theoretical Dense Coding

We have developed the theory of realistic quantum dense coding to some extent. We have calculated the state produced by degenerate non-collinear type-II down-conversion in a nonlinear BBO crystal given in Eq.(2.5.21). The theory of imperfect detectors has already been developed in chapter 2. Using the theory for experimental dense coding we calculated the hypothetical probability Eq.(4.3.29) by considering

ideal detectors at Alice's Bell state analyzer and we showed that our results in case of ideal detection gives the maximum probability with for a given value of  $\chi = 1$  and this probability decreases as the number of photon striking at the detector increases.

The methods provided in this dissertation provide the base components needed to develop a model that will determine the best source and detector efficiencies for use in an entanglement swapping and dense coding system. We have made a distinction between photon-number discriminating detectors and threshold detectors and it is shown that threshold detectors are more realistic as compared to photon number discriminating detectors. In developing the theory of realistic entanglement swapping, the actual quantum state after entanglement swapping and the probability with which this state exists are calculated. The original work which we have presented in this dissertation is a realistic model of experimental dense coding up to some extent. We calculated the state generated by these PDC sources in this process and the hypothetical probability in ideal case scenario. The results which come out from both processes have close resemblance with experimental results.

In future considerations, there is need to calculate the actual probability of the state detected in dense coding process in a realistic case. The study of variation in channel capacity in this case by taking into account all the inefficiencies present in the sources, detectors and line losses etc. would also be interesting. This work will be worth analyzing in view of promising technology advancements in research on quantum communication.

# References

- [1] S. J. Freedman and J. S. Clauser, Phys. Rev. Lett. **28**, 938 (1972).
- [2] M. Laméhi-Rachti and W. Mittig, Phys. Rev. D **14**, 2543 (1976); E. Hagley, X. Maitre, G. Nogues, C. Wunderlich, M. Brune, J. M. Raimond, and S. Haroche, Phys. Rev. Lett. **79**, 1 (1997).
- [3] A. Scherer, R. B. Howard, B. C. Sanders and W. Tittel, Phys. Rev. A **80**, 062310 (2009).
- [4] Jian-Wei Pan, D. Bouwmeester, H. Weinfurter, and A. Zeilinger, Phys. Rev. Lett. **80**, 3891 (1998).
- [5] F. Sciarrino, E. Lombardi, G. Milani, and F. De Martini, Phys. Rev. A **66**, 024309 (2002).
- [6] C. H. Bennett and S. J. Wiesner, Phys. Rev. Lett. **69**, 2881 (1992).
- [7] C. H. Bennett, G. Brassard, C. Crépeau, R. Jozsa, A. Peres, and W. K. Wootters, Phys. Rev. Lett. **70**, 1895 (1993).
- [8] C. H. Bennett, D. P. DiVincenzo, Nature. **404**, (2000).
- [9] J. Preskill, *Lecture notes on Quantum Information and Computation*, (1998).
- [10] K. Mattle, H. Weinfurter, P. G. Kwiat and A. Zeilinger, Phys. Rev. Lett. **76**, 25, (1996).
- [11] A. K. Ekert, Phys. Rev. Lett. **67**, 661 (1991).
- [12] D. C. Burnham and D. L. Weinberg, Phys. Rev. Lett. **25**, 84 (1970).

- [13] P. G. Kwiat, K. Mattle, H. Weinfurter, A. Zeilinger, A. V. Sergienko, and Y. H. Shih, *Phys. Rev. Lett.* **75**, 4337 (1995).
- [14] H.J. Briegel, W. Dr, J. I. Cirac, and P. Zoller, *Phys. Rev. Lett.* **81**, 5932 (1998).
- [15] R. B. Howard, M.Sc Thesis, *University of Calgary* (2009).
- [16] V. Scarani, H. B. Pasquinucci, N. J. Cerf, M. Duisek, N. Lutkenhaus, M. Peev, September **19**, (2008).
- [17] <http://www.ucd.ie/speclab/UCDSOPAMS/peoplehtml/quantumoptics2006/lecture5.pdf>
- [18] P. Grangier, G. Roger and A. Aspect, *Europhys. Lett.* **173**, 1 (1986).
- [19] H. Weinfurter and A. Zeilinger, *Quantum Communication* (Springer, Berlin/Heidelberg, 2001).
- [20] A. Zeilinger, *Dance of the Photons, Farrar, Straus and Giroux*, p. 205. (New York, 2010).
- [21] D. R. Truax, *Phys. Rev. D* **31**, 1988 (1985); C. C. Gerry, *Phys. Rev. A* **31**, 2721 (1985); K. Wodkiewicz and J. H. Eberly, *J. Opt. Soc. Am. B* **2**, 458 (1985).
- [22] B. Yurke, S. L. McCall and J. R. Klauder, *Phys. Rev. A* **33**, 4033 (1986).
- [23] C. Gerry, P. Knight, *Introductory Quantum Optics* (Cambridge University Press, 2005).
- [24] M. W. Hamilton, *Am. J. Phys.* **68**, 186 (2000).
- [25] F. Zappa, A. Lacaïta, S. Cova, and P. Webb, *Optics Letters*, **19**, 846 (1994).
- [26] S. D. Bartlett and B. C. Sanders, *Phys. Rev. A* **65**, 042304 (2002).
- [27] J. G. Rarity and P. R. Tapster, *Phys. Rev. Lett.* **64**, 2495 (1990).
- [28] M. Lamehi-Rachti and W. Mittig, *Phys. Rev. D* **14**, 2543 (1976).

- [29] E. Hagley, X. Matre, G. Nogues, C. Wunderlich, M. Brune, J. M. Raimond, and S. Haroche, *Phys. Rev. Lett.* **79**, 1 (1997).
- [30] S. Bose, V. Vedral, and P. L. Knight, *Phys. Rev. A* **57**, 822 (1998).
- [31] H. de Riedmatten, I. Marcikic, J. A. W. van Houwelingen, W. Tittel, H. Zbinden and N. Gisin, *Phys. Rev. A* **71**, 050302(R) (2005).
- [32] J. F. Clauser, M. A. Horne, A. Shimony, and R. A. Holt, *Phys. Rev. Lett.* **23**, 880 (1969).